

Chapter 4

Smart Metering Systems Based on Power Line Communications



José A. Cortés and J. Miguel Idiago

Abstract In recent years, the electricity grid has experienced a significant transformation in the generation side, with an increasing use of energy sources (renewable) that have a more decentralized structure and unpredictable availability than conventional ones. Similarly, the expected penetration of electric vehicles would considerably change the consumption patterns. These new circumstances require an improved monitoring and control of the electricity grid assets, and smart metering is a key element to achieve both ends. While there are many communication technologies for smart metering applications, power line communications (PLCs) have proven to be a cost-effective solution in a large number of scenarios. Moreover, it provides distribution system operator (DSO) a proprietary communication network and innately integrates the sensing and communication functionalities. Consequently, it has become the predominant smart metering technology in the EU and China, among others. In the last decade, several industrial alliances and standardization bodies have developed a number of narrowband PLC (NB-PLC) systems particularly tailored for smart metering applications. They implement a relay network that connects the smart meters to the data concentrator located in the medium voltage to low voltage (MV/LV) transformer stations. The latter are connected to the management center using different technologies, among which broadband PLC (BB-PLC) has proven to be a suitable one. The bit rate of the resulting shared medium provided by NB-PLC ranges from tens to hundreds of kilobit/s, which currently suffices for reading the energy consumption of 100 smart meters in less than 15 min.

Keywords Smart metering · High-data rate narrowband PLC · CENELEC-A band · FCC band

J. A. Cortés (✉)

Departamento de Ingeniería de Comunicaciones, Escuela Técnica Superior de Ingeniería de Telecomunicación, Universidad de Málaga–Campus de Excelencia Internacional Andalucía Tech, 29010 Málaga, Spain
e-mail: jaca@ic.uma.es

J. M. Idiago

PLC Software Engineer at Microchip Technology Inc, Polígono Puerta Norte, Torre C2, 50820 Zaragoza, Spain
e-mail: josemiguel.idiago@microchip.com

© Springer Nature Singapore Pte Ltd. 2019

E. Kabalci and Y. Kabalci (eds.), *Smart Grids and Their Communication Systems*, Energy Systems in Electrical Engineering, https://doi.org/10.1007/978-981-13-1768-2_4

4.1 Smart Metering Concept and Systems

Smart metering is an application that allows a distribution system operator (DSO) to remotely read the energy consumption of its customers, which is usually referred to as automatic meter reading (AMR), to obtain power quality information, to detect energy theft (usually referred to as meter tampering), and to perform some operations on the meter (e.g., connection/disconnection, meter programming) [15, 20, 61, 66]. In the European Union (EU), for instance, the term smart metering has even entered into the *acquis*, which is the body of law that state members accrue to the EU. Hence, Directive 2012/27/EC defines a smart metering or intelligent metering system as “an electronic system that can measure energy consumption, providing more information than a conventional meter, and can transmit and receive data using a form of electronic communication” [12].

Smart metering requires bidirectional communication links to the meters. The communication network used for this purpose is referred to as advanced metering infrastructure (AMI) and is the smart grid area that is currently focusing more deployment efforts. AMI enables additional applications like demand-side management (DSM) or distribution automation, which refers to the systems employed to remotely control the transformer substations [24, 61].

The communication requirements for smart metering applications have been quantified in Engage Consulting Limited [20]. For AMR, the estimated bit rate per smart meter is 3 kbit/s, assuming that the energy consumption value must be available at most 15 min after being requested [2]. Several technologies can be employed for this end. Wireless (radio frequency) is the most popular one in the United States of America (USA). Most wireless smart metering networks use cellular technologies like 2G/3G/4G, although mesh wireless networks based on the IEEE 802.16e are being also proposed. DSOs are generally reluctant to use public networks for AMI because of their cost and absence of priority (over other services) in case of network congestion. The lack of spectrum restrains DSOs from deploying wireless private networks. Digital subscriber line (DSL) technologies have been also employed for this purpose, although their high maintenance cost has prevented its massive deployment [66]. Power line communications (PLCs) and, in particular, the technology referred to as narrowband PLC (NB-PLC) have proven to be a cost-effective solution for many scenarios. Accordingly, it is the most widespread smart metering technology in the EU and China. NB-PLC provides a communication network that is under the absolute control of the DSO. It reuses the existing wired infrastructure; hence, the deployment costs are greatly reduced. Since a PLC transceiver may act both as a sensor and as a modem, PLC naturally integrates two key functions of the smart grid: sensing and communicating. Moreover, NB-PLC is particularly suited for applications where a low and bounded latency is crucial, such as teleprotection [24]. It can be also used for retrieving the physical topology of the power grid, which is sometimes unknown by the DSO and that can be used for online monitoring of grid elements such as loads and lines [1].

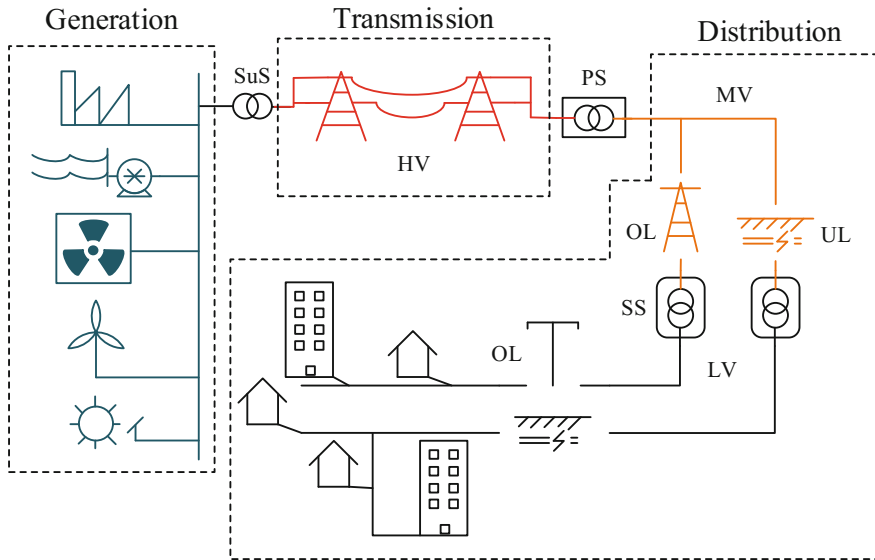


Fig. 4.1 Simplified scheme of the electricity grid

Structure of the electrical grid

The electricity system consists of the three main domains as shown in Fig. 4.1, namely generation, transmission, and distribution. Transition between domains is performed by transformer stations. Firstly, a step-up substation (SuS) raises the voltage given by the generation plants up to hundreds of kV, which is referred to as high voltage (HV) to reduce transmission loss. In primary substations (PSs), this HV is further reduced to tens of kV, which is known as medium voltage (MV). By means of MV overhead lines (OLs) or underground lines (ULs), electricity reaches the secondary substations (SSs), where the voltage is further lowered to 230 V/120 V, depending on the country. This is referred to as low voltage (LV).

HV and MV lines shown in Fig. 4.1 are three-phase ones. LV lines departing from the SS have three conductors (one for each phase) plus a neutral one. Residential customers are generally fed by a single phase (and neutral), while more energy-consuming customers are read by three-phase lines.

The MV and LV segments are probably the most heterogeneous part of the electricity grid. For instance, in Europe, the LV one consists of OL and UL and each SS typically consists of 2–3 transformers that serve 150–300 customers with distances typically lower than 300 m. By contrast, in North America, most LV lines are OL and each SS typically serves 10–15 customers [61]. Moreover, the frequency of the mains signal is 50 Hz in Europe and most parts of Asia and 60 Hz in most American countries.

4.2 PLC Systems for Smart Metering

Categorization of PLC technologies

The employed bandwidth is the most distinctive feature of the different PLC technologies. In fact, electromagnetic compatibility (EMC) regulations do also classify PLC technologies according to this criterion, as it will be shown later in this chapter. The useful categorization in [24] distinguishes three PLC technologies:

- Ultra narrowband (UNB): Refers to systems using frequencies below 3 kHz, which yields large operational ranges, and conveying bit rates around 100 bit/s. Existing systems employ proprietary solutions and have been used for decades in smart metering applications.
- Narrowband (NB): It refers to systems operating in frequencies up to 500 kHz. Within this group, two different technologies can be distinguished:
 - Low data rate (LDR): Based on single carrier modulations are able to convey a few kbit/s. They have been traditionally used in smart metering applications and in home automation ones. Examples of these groups are the IEC 61334-5, based on frequency shift keying (FSK) and spread-FSK modulations and X10 specifications.
 - High data rate (HDR): These systems employ multicarrier modulations and attain hundreds of kbit/s. They have been developed in the last decade and seem to be the most cost-effective solution for smart metering applications. The most successful ones were initially developed by industrial alliances, such as PowerLine Intelligent Metering Evolution (PRIME) Alliance and G3-PLC Alliance, and then standardized by the ITU (International Telecommunications Union) under ITU-T Rec. G.9904 [40] and ITU-T Rec. G.9903 [39], respectively. Others, fully developed by standards developing organizations, like the ITU-T Rec. G.9902 (G.hnem) [38] and the IEEE 1901.2 [33], have not yet commercially succeeded.
- Broadband (BB): This group, also referred to as broadband power line (BPL), encompasses a large variety of systems using the frequency band above 1.6 MHz and up to 250 MHz. Most of them are based on multicarrier modulations, and the latest versions include multiple-input multiple-output (MIMO) technology, like the IEEE 1901 [34], the ITU-T G.hn [41–43], and the HomePlug AV2 [27]. This technology has been designed for high bit rate applications like local area networking in small offices and homes. Within the smart grid, they are used as telecommunication backbone to connect the SS using the MV lines [46], but it is being recently proposed also for the last mile of smart metering applications, i.e., the connection of the SS to the smart meter.

At this moment, NB-PLC is by far the most common PLC technology for the last mile part of smart metering networks. Therefore, henceforth we will concentrate on the study of this technology.

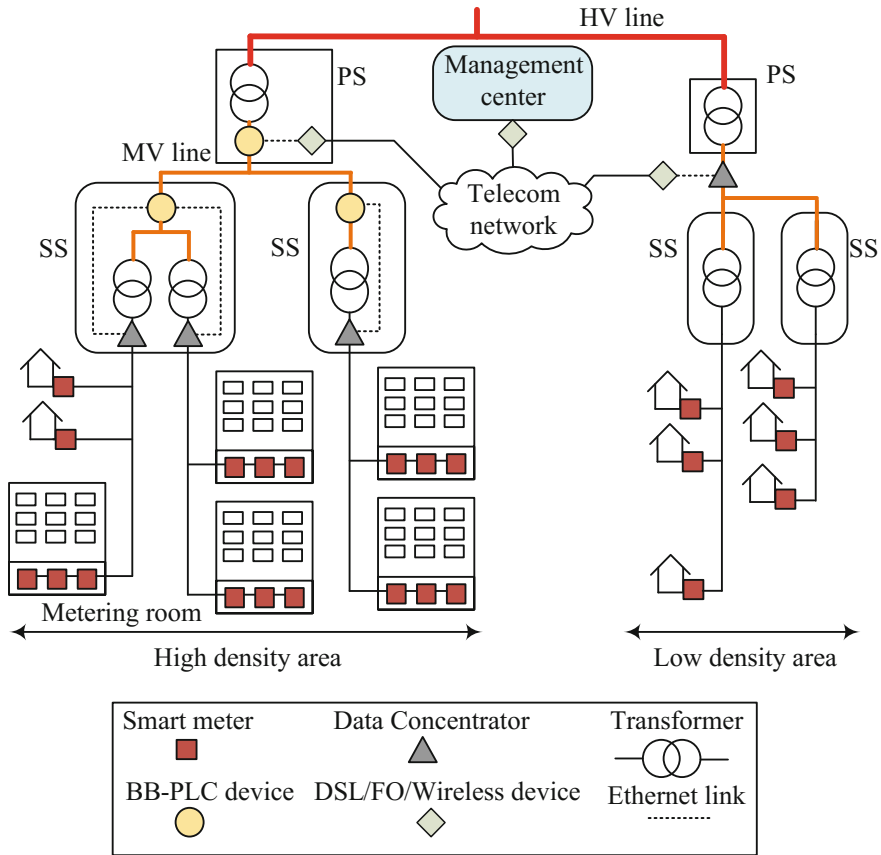


Fig. 4.2 Simplified scheme of a smart metering network

Structure of PLC smart metering systems

Figure 4.2 depicts the system model of an NB-PLC-based smart metering network. The management center is the element from which smart meters are controlled and where energy consumption values are reported. Interestingly, information retrieved from the smart meters can be also used for other functions such as power quality and outage management, transformer load management, and power grid tomography, which integrates with the DSO geographic information system [49].

The management center is connected to the SS by means of a backbone network. This may consist of a mixture of technologies like DSL, fiber optics (FO) communications, wireless (radiofrequency) technologies, or even BB-PLC, which has proven to be a feasible alternative for this purpose [61]. Finally, the last mile segment of the network connects the smart meters to the data concentrator (DC). The latter may be located at two different places, depending on the number of customers connected to the MV/LV transformer. In scenarios where the number of customers is high, the DC

is usually placed at the LV side of the transformer. This is the case of most European urban areas. However, there are countries where the number of customers connected to each transformer is very low, even in urban areas, e.g., in the USA. Since DCs are expensive, placing them in the LV side is not a cost-effective solution.

The location of the DC is a key element for the selection of the NB-PLC solution to be employed because many of them are unable to provide connectivity through transformers. As it will be discussed further in this chapter, this is the case of the systems that work in the frequency range below 95 kHz. In these circumstances, even if BB-PLC is used in the backbone network, the connection between the BB-PLC device and the NB-PLC one is generally done by means of an ethernet link, bypassing the transformer as indicated in Fig. 4.2.

An important aspect related to NB-PLC-based systems is the signal injection method [60]. At the customer side, single phase is generally the only possibility, since homes are usually fed by using a single phase. At the transformer side, while three-phase injection is possible, single-phase injection is currently the most widespread one; i.e., NB-PLC systems do not currently explore the MIMO nature of the network. This is contrast to the BB-PLC case, where the latest standardized systems do all include MIMO techniques.

Application protocols for smart metering

At application level, smart metering systems vary a lot depending on the utility. Protocols like ANSI C 12.18, that was designed to work over optical port but that was lately extended in the ANSI C 12.21 to work over public switched telephone network (PSTN) modems, were widely used by American utilities. Similarly, Euridis (IEC 1142 and the latest version IEC 62 056-31), that was designed to work over twisted pair cables for the remote reading of residential meters, was used by French utilities. However, nowadays the most widely accepted protocol for utility meter data exchange is DLMS/COSEM [29–31].

The DLMS/COSEM specification is defined in the set of standards IEC 62056. DLMS is the acronym for “device language message specification” and consists of a suite of protocols [13]. COSEM is the acronym for “companion specification for energy metering” and consists of a set of specifications that define the transport and application layers of the DLMS protocol. DLMS defines general concepts for the communication between entities, while COSEM establishes concrete rules for exchanging the data related to the concepts defined in DLMS.

The DLMS User Association defines the protocols into a set of four specification documents, namely as the “colored books”:

- Blue Book: It describes the COSEM meter object model and the object identification system.
- Green book: It describes the architecture and protocols to transport the model.
- Yellow book: It describes the conformance testing process.
- White book: It holds the glossary of DLMS/COSEM terms.

DLMS/COSEM is designed following the client/server model, where meters generally act as servers. When the utility wants to get information from a meter, the

DC or whatever system or device in charge of retrieving the information from the meter establishes a connection to the DLMS/COSEM server running in the meter. DLMS/COSEM requires an “association” process to bring security and authentication features. Once a client correctly establishes an association with the server, it can read or write any of the object identification system (OBIS) defined in the meter.

Several COSEM OBIS are defined to hold management and configuration data, to manage access rights and security, to set up communication interfaces, for time- or event-based control. COSEM OBIS are designed to be used for metering and controlling electrical, gas, water, heat energy and many other type of meters COSEM OBIS allow modelling a large range of metering and control functions like billing, payment, load profiling, power quality measurement, revenue protection, customer information, load and supply control. Management functions include configuration, parametrization, firmware update, security, meter and communication channel supervision.

4.2.1 EMC Regulation

The frequency band and the signal level injected by PLC systems is constrained by EMC regulations, which are intended to ensure coexistence with other communication systems. This is done by limiting both the conducted and radiated emissions. Radiated emissions are due to the common mode (CM) currents, also known as antenna currents. Despite PLC signals are applied in a differential manner between two conductors, causing differential mode currents, CM currents also appears due to the asymmetries in the network [65]. Unlike differential mode currents, which flow in opposite direction, CM ones flow in the same direction. Hence, while the former radiates electric fields that tend to cancel, the generated fields due to the latter tend to add, causing significant radiated electromagnetic interference (EMI). The magnitude of the radiated EMI due to the CM becomes important when the length of the radiating structure is comparable to the wavelength of the conducted signal. For frequencies below 500 kHz, this requires cable lengths larger than 600 m. Hence, radiated emissions are an important concern only in BB-PLC and are not included in NB-PLC regulations.

Regarding conducted emissions, since the power injected by a PLC device depends on the impedance of the power line network, conducted emissions test is carried out using an artificial mains network (AMN), also known as line impedance stabilization network (LISN) [32]. The AMN/LISN provides a well-known impedance to the PLC device and filters out the noise coming from the power line network. They also allow measuring both differential mode and CM currents.

EMC regulations applicable to PLC vary with the country; however, most of them use the standards produced by the Comité International Spécial des Perturbations Radioélectriques (CISPR) as the base to develop their own norms. The CISPR is part of the International Electrotechnical Commission (IEC), an international standards

Table 4.1 Summary of frequency bands and applicable EMC regulation to PLC systems in the EU, the USA and Japan

State	Frequency range	EMC regulation
EU	3–148.5 kHz	EN 50065
	150–500 kHz	Without specific regulation. Directive 2004/108/EC can be applied
	1.6065–30 MHz	EN 50561-1 (only indoor PLC)
	30–87.5 MHz	EN 50561-3 (only indoor PLC)
USA	9–490 kHz	Code of Federal Regulations, Title 47, Part 15
	1.705–80 MHz	
Japan	10–450 kHz	STD-T84
	2–30 MHz	See ITU-T Rec. SM.1879-2

organization whose members are called national committees, which are comprised of the nations' public and private actors interested in electrotechnical issues.

In the European Union (EU), the Comité Européen de Normalisation Électrotechnique (CENELEC) uses CISPR standards to produce the European harmonized standard that have to be adopted by EU members. For instance, the EN 55022 [19] is derived from the CISPR 22. In the USA, EMC issues are regulated by the Federal Communications Commission (FCC), while in Japan this role is played by the Association of Radio Industries and Businesses (ARIB). The latter are also adopted by other Asian countries. The following subsections discuss the allowed frequency bands and the applicable EMC norms in various countries, which are summarized in Table 4.1 [2, 25].

NB-PLC

Figure 4.3 summarizes the frequency bands allocated to NB-PLC technology in the EU, the USA, and Japan.

In the EU, PLC in the 3–148.5 kHz range is regulated by the EN 50065-1 [16]. It defines four sub-bands, which in Fig. 4.3 have been named using the nomenclature employed in the previous versions of this norm. The 3–95 kHz range, traditionally referred to as sub-band A, is reserved for utilities. Within the 9–95 kHz band, the differential mode voltage of the signals whose bandwidth exceeds 5 kHz is limited to 134 dB μ V and the power spectral density (PSD) to 120 dB μ V/200 Hz,¹ measured using a given AMN. For the HDR NB-PLC systems currently employed in smart metering applications, the former constraint is the most restrictive one. For instance, the bandwidth employed by the systems defined in the ITU-T Rec. G.9904 (PRIME)

¹The EN 50065-1 specifies the PSD constraint as the voltage level measured in a 200 Hz band. This can be translated to the more common dB μ V/ $\sqrt{\text{Hz}}$ as dB μ V/ $\sqrt{\text{Hz}}$ = dB μ V/200 Hz – 23.01.

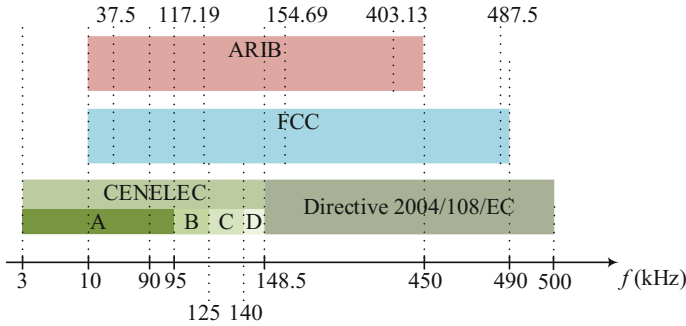


Fig. 4.3 Regulated frequency bands for NB-PLC systems in some countries

and ITU-T Rec. G.9903 (G3-PLC), that will be discussed in Sect. 4.2.3, is approximately 47.36 and 56.25 kHz, respectively. Injecting a signal level of 134 dB μV yields 110.26 dB $\mu\text{V}/200\text{ Hz}$ and 109.51 dB $\mu\text{V}/200\text{ Hz}$, respectively. Hence, injecting 120 dB $\mu\text{V}/200\text{ Hz}$ would have exceeded the 134 dB μV constraint.

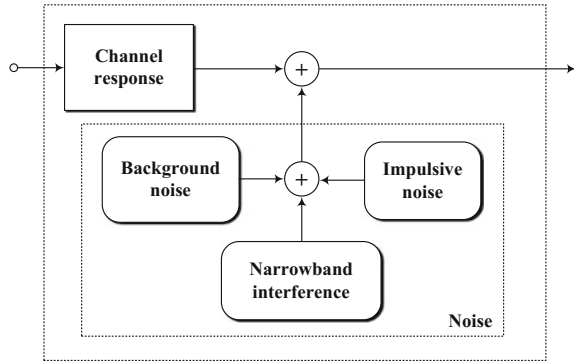
There is no specific regulation for PLC in the 150–500 kHz. Hence, in principle, EMC limits defined in the EN 55022 apply [19]. This norm sets limits to the spurious signals injected by information technology equipment into the mains port (for power supply) and the telecommunication port. Since a single port is used for both purposes in PLC, these limits are too stringent. However, since 2004 the Directive 2004/108/EC manufacturers are permitted to assess the EMC of their products either by means of a European harmonized standard or by using their own procedures [11]. The latter have to be certified by means of an independent notified body. The IEEE P1901.2 specification [33], for instance, proposes a procedure for such end.

In the USA, PLCs in the 9–490 kHz band are regulated by the Code of Federal Regulations, Title 47, Part 15, issued by the FCC [21]. It clearly distinguishes two types of PLC systems, referred to as “power line carrier systems” and “carrier current systems”. The latter are intended for connecting the distribution substations to the customer, e.g., for smart metering purposes. These systems have to fulfill the in-band radiated emissions and the out-of-band conducted emissions limits defined in sections 15.209(a) and 15.107(c), respectively. No in-band conducted limited is set, contrary to the EN 50065-1.

In Japan, PLC in the 10–450 kHz band is regulated by the STD-T84 [64] issued by the ARIB. It sets in-band and out-band conducted emission limits. Regarding the former, it limits the PSD to 30 mW/10 kHz (134 dB $\mu\text{V}/\sqrt{\text{Hz}}$) for transmissions below 200 kHz and to 10 mW/10 kHz (130 dB $\mu\text{V}/\sqrt{\text{Hz}}$) when the transmitted band exceeds 200 kHz [2], where power is measured over a 10 Ω load.

Despite the information regarding EMC regulations concerned with NB-PLC in China is still somehow inaccessible, it is known that there exist deployed systems (all of them proprietary solutions) operating below 95 kHz and others that work up to 422 kHz [44].

Fig. 4.4 LV NB-PLC channel model



BB-PLC

In the EU, indoor BB-PLC is regulated by the EN 50561-1 [17], for frequencies in the 1.6065–30 MHz band and by the EN 50561-3 for frequencies in the 30–87.5 MHz range [18]. Both norms set limits for the conducted and radiated emissions. Moreover, the EN 50561-1 also mandates the implementation of a cognitive frequency exclusion mechanism that creates notches in the passband when a broadcast service is detected. The EN 50561-2, which regulates outdoor BB-PLC, is not yet approved.

In the USA, the Code of Federal Regulations, Title 47, Part 15, regulates both indoor and outdoor BB-PLC (BPL, as designated by the FCC) in the frequency range 1.705–80 MHz. It defines limits for the conducted and radiated emissions.

In Japan, BB-PLC can operate only in the frequency range 2–30 MHz [36]. Limits for both the radiated and CM conducted emissions are defined (in most cases, they are taken from the CISPR 22).

4.2.2 Channel Characteristics

This section describes the characteristics of the NB-PLC channel between the SS and the customer point of supply. Figure 4.4 depicts a suitable channel model. The channel response is time and frequency selective. Time variations occur in the long term (hours), e.g., due to the pattern of connection/disconnection of the electrical appliances, and in the short term due to the periodicity of the mains. Hence, PLC channels can be modeled as a linear and periodically time-varying (LPTV) filter whose frequency is generally twice the one of the mains. However, the linear and time-invariant (LTI) approach suffices for NB-PLC systems, where the used band is relatively narrow. Noise in PLC consists of three main terms: impulsive noise, background noise, and narrowband interference (NBI) [8].

Channel response

The response of the NB-PLC channels in the LV distribution network can be modeled as depicted in Fig. 4.5. The three phases of the transformer output are labeled as R, S,

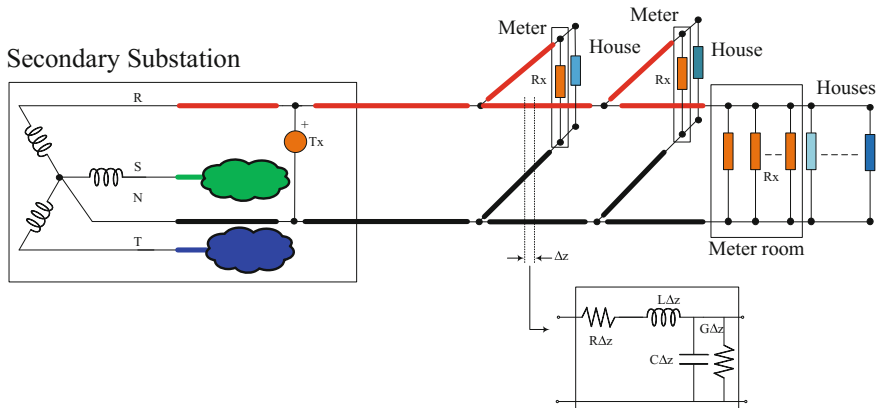


Fig. 4.5 Modeling of the LV distribution network from the NB-PLC channel response perspective

and T (other common designations are L1, L2, and L3). Currently, NB-PLC devices are connected in a single-input single-output (SISO) manner between one phase and the neutral (N) conductor. For simplicity, only the connection corresponding to the R phase is shown. The transmitter is modeled as a voltage generator (the impedance of NB-PLC transmitters is generally lower than 500 mΩ) and the receiver by means of an impedance. From the NB-PLC channel response perspective, a whole house can be modeled by its input impedance.

As a rule of thumb, the cables that connect the transmitter to the receiver behave as transmission lines when their length is larger than $\lambda/10$, where λ is the wavelength of the transmitted signal. For the higher frequency of the CENELEC A band (95 kHz) and assuming a propagation speed equal to 0.8 c, this yields a cable length of about 253 m, which is larger than the actual length of most LV lines in residential areas in the EU [52]. Hence, the skin effect, that yields a low-pass profile to the frequency response, is not a main issue for NB-PLC channels in these circumstances, except for very long links. For the edge frequencies of the range 150–450 kHz, the aforesaid length reduces to 160 m and to 53 m, respectively. Hence, NB-PLC channels are likely to be affected by the skin and the multipath effect, especially in rural areas, where LV lines are longer than in urban ones.

Figure 4.6 depicts the amplitude response of six channels measured in Spain in the 40–91 kHz band in three different environments (urban, semiurban, and rural). Similarly, Fig. 4.7 shows the amplitude response of six channels measured in the same scenarios but in the 150–490 kHz range. As seen, no clear low-pass profile is observable. Similarly, the multipath propagation effect, which causes notches in the frequency response, is not an important concern. In these circumstances, the loading effect from the indoor power line networks becomes much more important.

From a communication perspective, the most informative channel response parameters are the average attenuation and the delay spread, or its frequency domain counterpart, the coherence bandwidth [57]. The latter are particularly useful for the

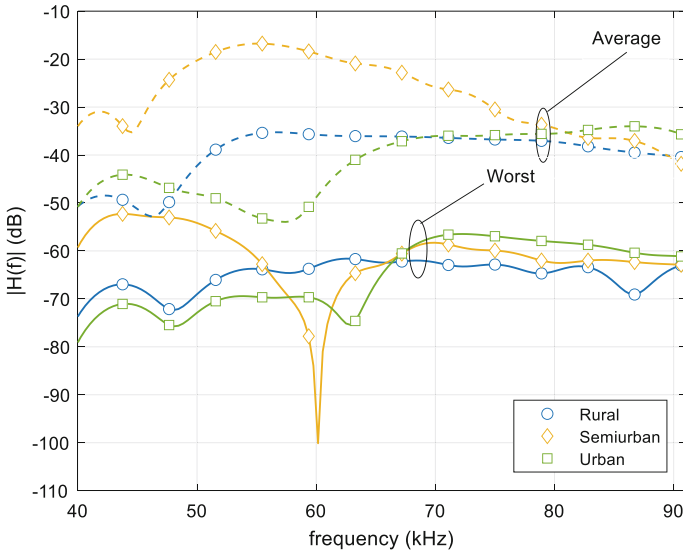


Fig. 4.6 Amplitude response of LV channels measured in Spain in the 40–91 kHz band. Courtesy of Microchip Technology Inc.

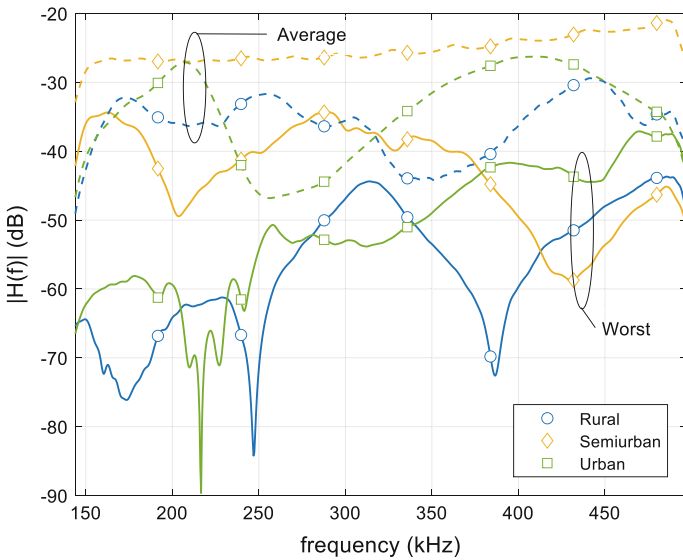
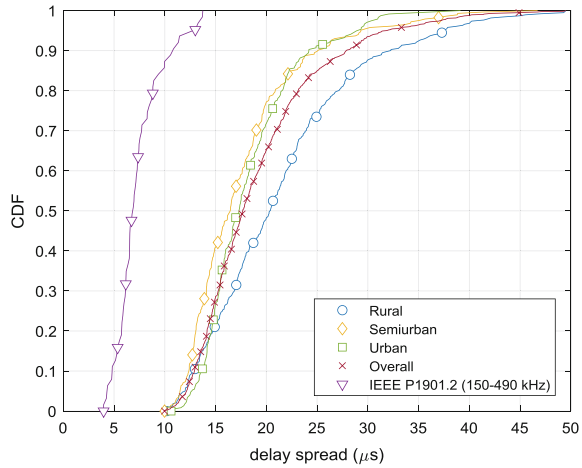


Fig. 4.7 Amplitude response of LV channels measured in Spain in the 150–490 kHz band. Courtesy of Microchip Technology Inc.

design of orthogonal frequency division multiplexing (OFDM) systems. Hence, the cyclic prefix must be longer than the channel impulse response length in order to

Fig. 4.8 CDF of the delay spread of measured and modeled channels in the 40–91 and 150–490 kHz bands, respectively. Adapted by the authors from Cortés et al. [9]



avoid intersymbol interference and intercarrier interference (ISI and ICI). However, since a precise measure of the impulse response length is not feasible in actual channels, the root mean square (RMS) measure given by the delay spread provides a serviceable information for determining the cyclic prefix length. Even when neither ICI nor ISI occurs, selecting the carrier spacing of the OFDM system narrower than the coherence bandwidth is beneficial for physical layer tasks such as channel estimation.

Figure 4.8 depicts the cumulative distribution function (CDF) of the delay spread of 106 channels measured in Spain in the frequency band 40–91 kHz in three different scenarios: urban, semiurban, and rural [9]. Unfortunately, while extensive measurements campaigns have been accomplished in the 150–500 kHz band, all of them are proprietary. Hence, statistics are not publicly available. The IEEE P1901.2 specification proposes a channel model for this band. Although there are no published results that assess the suitability of this model by comparing its results to measurement, they can be used, at least, to obtain prospective values. Accordingly, statistics obtained from 300 channels generated according to this model in the 150–490 kHz band are shown in Fig. 4.8. As seen, the impulse responses of the channels in the 150–490 kHz range are shorter than in the 40–91 kHz one.

Figure 4.9 shows the CDF of the coherence bandwidth² and the average attenuation of the channels as shown in Fig. 4.8. As seen, rural channels have larger delay spread values than urban and semiurban ones. This is likely due to the low-pass behavior that appears in very long links. However, despite this profile, urban channels tend to be more attenuated due to the more branched structure of the network. Although not shown in the figure, there is no correlation between the delay spread and the average attenuation, as it happens in indoor BB-PLC channels, where more

²Computed as the frequency separation for which the spaced-frequency correlation function falls down to 0.9 [57].

Fig. 4.9 CDF of the coherence bandwidth and the average attenuation of measured and modeled channels in the 40–91 and 150–490 kHz bands, respectively. Adapted by the authors from Cortés et al. [9]

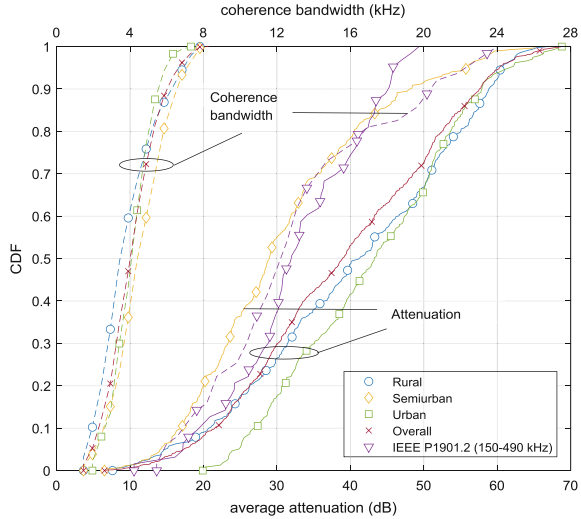


Table 4.2 Summary of the measured channel response parameters in the 40–91 kHz range and of the modeled ones in 150–490 kHz band

Parameter	Percentile					
	10%		50%		90%	
	40–91 kHz	150–490 kHz	40–91 kHz	150–490 kHz	40–91 kHz	150–490 kHz
Delay spread (μ s)	12.92	4.81	17.67	6.83	27.88	10.77
Coherence bandwidth (kHz)	2.28	6.90	4.01	12.20	6.23	20.36
Average attenuation (dB)	21.54	19.38	38.93	31.94	57.58	45.15

attenuated channels use to have larger delay spread values. Table 4.2 summarizes the 10, 50, and 90% percentiles of the three parameters for the overall set of measured channels in the 40–91 kHz band the modeled ones in the 150–490 kHz range. Their comparison can only provide prospective characteristics, since we are contrasting measured with modeled channels. Having this precaution in mind, channels seem to be more harmful in the 40–91 kHz band than in the 150–490 kHz range. Parameters given in Table 4.2 will be helpful to assess the matching of the physical layer of the main NB-PLC systems to the channel characteristics.

Input impedance

The input impedance of the power line generally increases with frequency. According to the results given in [9], the frequency-averaged modulus of the impedance in the

40–91 kHz range reaches maximum values of tens of ohms. The minimum ones are about 1Ω and the median (percentile 50%) around 5Ω .

Such low impedance values pose a twofold problem for NB-PLC systems. The first one is the difficulty of injecting signal levels of up to 5 V, as the ones allowed by the EN 500651 into such low impedance values [16]. The second one is the difficulty of making the transmitter impedance much lower than the input impedance of the power line network, i.e., on the order of a few $m\Omega$, which is in the range of the resistance of some printed circuit board traces or the transformers wiring. It should be noted that conjugate impedance matching is also technologically difficult because of the aforesaid frequency-selective behavior of the impedance and its large variation between locations.

Noise

As mentioned, NB-PLC consists of three different terms: impulsive noise, NBI, and background noise, which encompasses the remaining noise types not included in the previous categories [8].

Impulsive noise consists of three different terms:

- Periodic synchronous with the mains. It is a cyclostationary noise, synchronous with the mains and with a frequency of 50/100 Hz or 60/120 Hz, depending on the country. It appears either as impulses of considerable duration (hundreds of microseconds) and amplitude or as impulse trains in which the number of impulses and separation between them varies from cycle to cycle. Figure 4.10 depicts an example of this type of noise measured in Spain. It shows many noise impulses; however, a periodic component with two large amplitude impulses per mains cycle can be clearly observed. The first impulse appears at about $t = 10$ ms and the second at around $t = 15$ ms.
- Periodic asynchronous with the mains. It consists of impulse trains that always appear at the same instants of the mains cycle. Hence, it is also synchronous with the mains. However, the designation asynchronous is due to the fact that the separation between impulses, which is fixed, is not related to the mains period.
- Sporadic. It appears in a twofold manner: as isolated impulses with considerable amplitudes and widths and as impulse trains with arbitrary separation between the constituent pulses. Their distinctive feature is that they are completely asynchronous to the mains signal. An example of this component is shown in Fig. 4.11 at about $t = 22$ ms.

NBI consists of sinusoidal signals, in most cases with modulated amplitudes. Interestingly, in many cases the amplitude varies synchronously with the mains. Its PSD takes the form of narrow spectral lines with a much higher level than the remaining noise terms, as illustrated in Fig. 4.12.

While the aforementioned noise terms are common to both the 3–148.5 kHz and the 150–500 kHz, and even to the BB-PLC channel, all measurements campaigns accomplished in the 150–500 kHz band are proprietary. Hence, statistics are not publicly available. The IEEE P1901.2 specification provides a time and frequency analysis of a large number of measured registers and a corresponding noise model

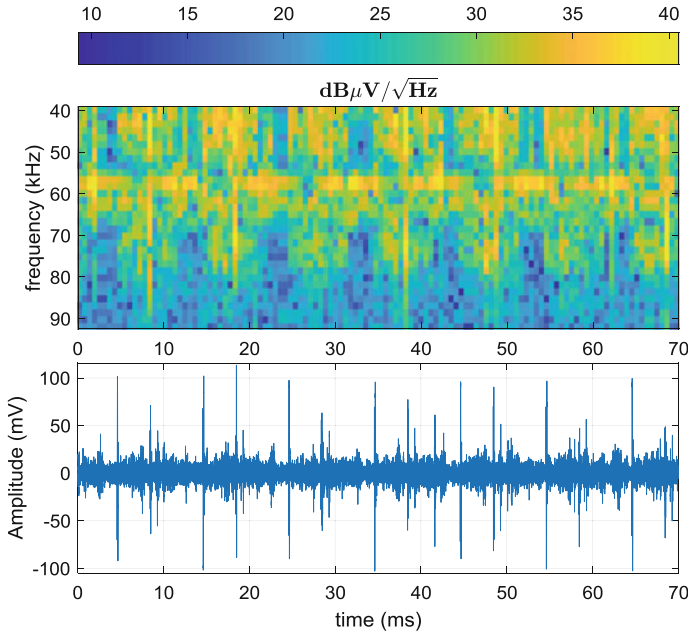


Fig. 4.10 Example of a noise register measured in Spain and its corresponding spectrogram. Courtesy of Microchip Technology Inc

for this band. Contrasting them with results given in [9], it seems that noise (and in particular, the background noise term) is less harmful in the 150–500 kHz band and in the 3–148.5 kHz one.

Noise pattern remains unchanged for several seconds or minutes during the day. During the late night, this period is much larger [28]. It is also interesting to mention that noise level at the transformer LV output generally exhibits larger variations along the mains cycle [5] and among phases [9] than at the customer site.

Except for the sporadic noise impulses, PLC noise can be regarded as cyclostationary. Hence, its time-averaged PSD³ can be computed and used, along with the channel attenuation values given in Table 4.2 to obtain prospective values of the signal-to-noise ratio (SNR). Figure 4.13 shows representative values of the PSD of a large set of noise registers measured in Spain in the 41–90 kHz range. The PSD of a “high” and a “low” level noise registers is depicted along with the average PSD (over the whole set of measurements). Let us consider that an NB-PLC signal with 50 kHz bandwidth and 134 dB μV (as defined in the EN 50065-1) is injected. Assuming an attenuation value of 40 dB and a noise PSD value of $-40 \text{ dB } \mu\text{V}/\sqrt{\text{Hz}}$, the resulting average SNR is 7 dB. It should be taken into account that this is an average value and that the bit error rate (BER) is dominated by the lower SNR values.

³For simplicity, this will be referred simply to as PSD.

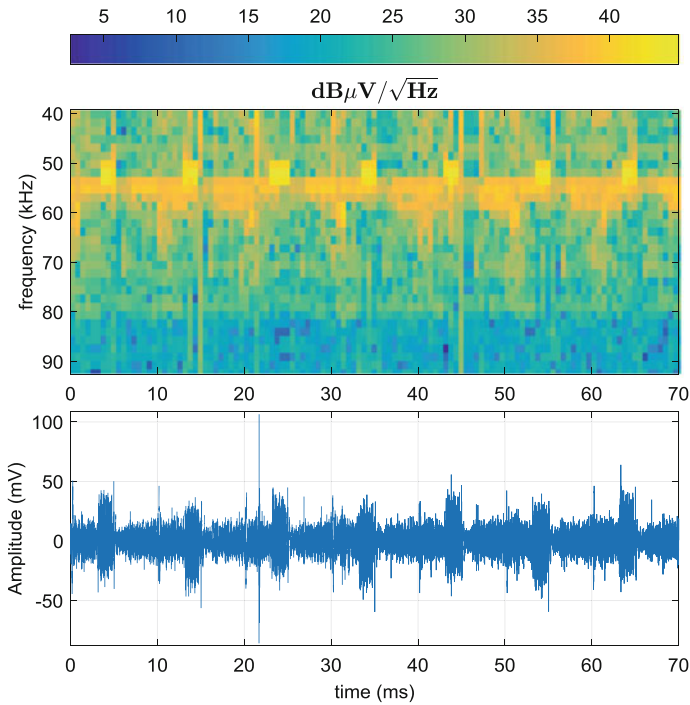


Fig. 4.11 Example of a noise register measured in Spain and its corresponding spectrogram. Courtesy of Microchip Technology Inc

MV/LV Transformers

In European smart metering networks, the DC is located at the LV side of the MV/LV transformer. However, as mentioned, in many North and South America regions the number of customer connected to each transformer is much lower. Since data concentrators are expensive, the architecture used in European networks is not cost-effective in the latter scenario.

Nevertheless, placing the data concentrator at the MV side of the transformer is not straightforward because of the channel response of the transformer. Measurements reported in [10] and [51] suggest that the attenuation is generally much higher in the 30–90 kHz than in frequencies above 150 kHz. In fact, some of the HDR NB-PLC systems that will be described in this chapter are targeted at allowing communications through the MV/LV transformer.

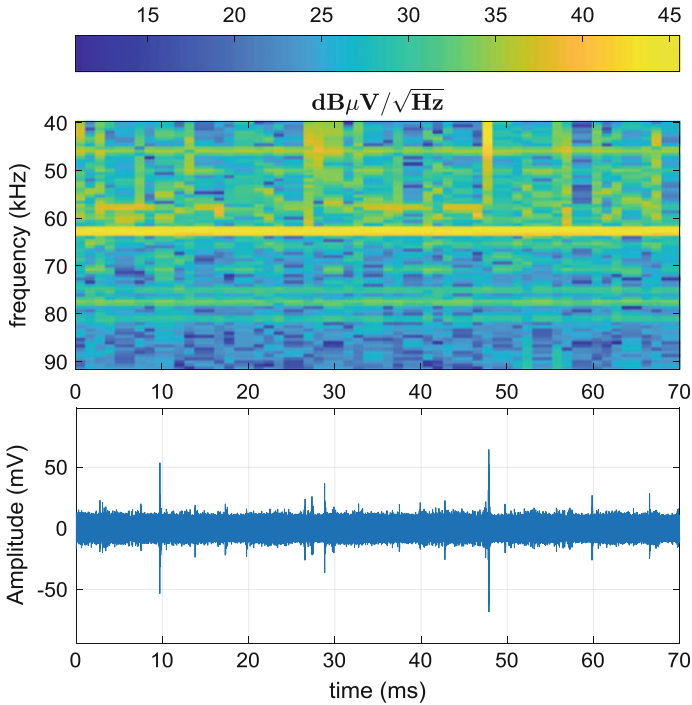


Fig. 4.12 Example of a noise register measured in Spain and its corresponding spectrogram. Courtesy of Microchip Technology Inc

4.2.3 Standardized and Industrial Systems

In the context of PLC-based smart metering networks, HDR NB-PLC is the most widespread technology for connecting the SS to the smart meter. While BB-PLC is being also proposed for this purpose, its main role in current deployments is as backbone for connecting SS. This backbone is then connected, e.g., by means of DSL or FO technologies to the central system [62]. Two BB-PLC systems can be used for this purpose, the IEEE P1901 and the ITU-T G.hn. Since these standards were released in 2010, legacy BB-PLC systems can be also found in networks deployed before this year [62]. This subsection concentrates on the description of the HDR NB-PLC systems.

At the time of writing this chapter, there are four standardized HDR NB-PLC systems. Two of them, commercially known as PRIME v1.3.6 [54] and G3-PLC [22], were initially specified by the homonymous industrial alliances and then standardized by the ITU-T in 2012 under Recs. G.9904 and G.9903, respectively. The other two systems are defined in the ITU-T Rec. G.9902, commonly referred to as G.hnem (released in 2012) and the IEEE P1901.2, released in 2013. The PSD limits for the ITU-T Rec. G.9902 (G.hnem), the ITU-T Rec.G.9903 (G3-PLC), and the ITU-T Rec.

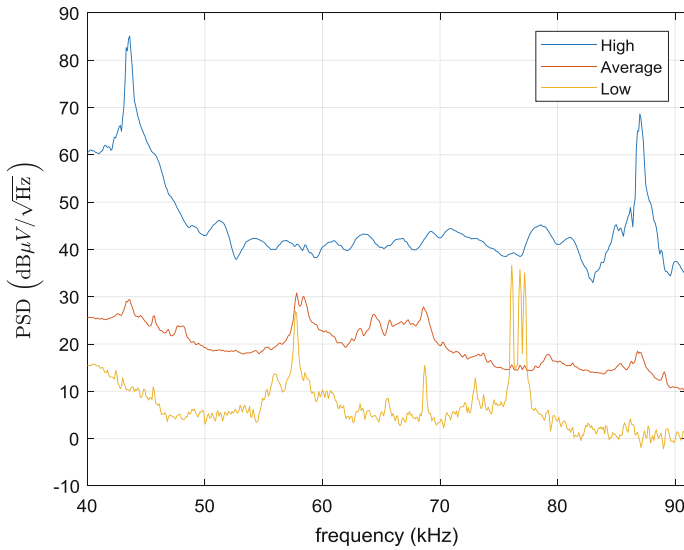


Fig. 4.13 Representative PSD values of the noise in the 40–91 kHz band. Adapted by the authors from Cortés et al. [9]

G.9904 (PRIME) is defined in the ITU-T Rec. G.9901 [37]. A new version of the PRIME system, referred to as PRIME v1.4, was made public in 2014 [56]. Table 4.3 highlights the main features of the aforementioned systems. It should be mentioned that, at this moment, neither the ITU-T Rec. G.9902 (G.hnem) nor the IEEE P1901.2 have commercially available devices. Moreover, not even a certification procedure is available.

4.2.3.1 ITU-T Rec. G.9904 (PRIME)

The PRIME Alliance, led by the Spanish DSO Iberdrola, released the PRIME v1.3.6 specification in 2008. It was intended to connect the smart meters to the DC located in the SS using the CENELEC A band. This was lately standardized as ITU-T Rec. G.9904 (PRIME) [40], which is the system described herein and the ITU-T Rec. G.9901 [37], which defines the PSD and the AMN to be used for measuring it. Figure 4.14 shows the reference model of the ITU-T Rec. G.9904 (PRIME).

It employs an OFDM-based physical layer (PHY) layer operating in the CENELEC A band. This has been further extended in PRIME v1.4 to 500 kHz to open new geographic markets.

From the point of view of the medium access control (MAC) layer, an ITU-T Rec. G.9904 (PRIME) network is composed of two kinds of devices: a single base node (BN) and multiple service nodes (SN). The BN is a key part of the system and sometimes is also referred as DC. The BN is generally placed in the low voltage side

Table 4.3 Summary of the standardized HDR NB-PLC systems

System	Bandplan	Modulation (number of bits/symbol)	FEC	Routing algorithm
ITU-T Rec. G.9904 (PRIME)	CENELEC A	Differential in frequency (1, 2, 3)	CC/uncoded	L2, proactive
PRIME v1.4	CENELEC A B C D + FCC + ARIB	Differential in frequency (1, 2, 3)	CC/uncoded	L2, proactive
ITU-T Rec. G.9903 (G3-PLC)	CENELEC A/B + FCC-H + ARIB	Differential in time (1, 2, 3) + coherent (opt)	RS + CC + RC	L2, reactive (LOADng)
IEEE P1901.2	G3 + FCC-Low + FCC-above-CEN + ARIB 1 + ARIB 2	Differential in time (1, 2, 3) + coherent (opt)	RS + CC + RC	No included in spec.
ITU-T Rec. G.9902 (G.hnem)	CENELEC A/B + FCC-1 + FCC-2 + FCC + ARIB	Coherent (1, 2, 4)	RS + CC + RC	Optional L2 (under study)

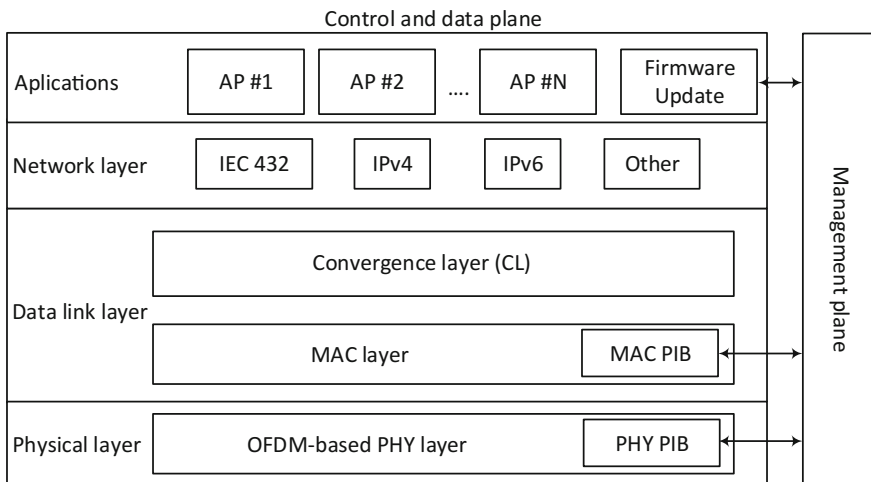


Fig. 4.14 Layer architecture of the ITU-T Rec. G.9904 (PRIME) system. Adapted by the authors from ITU-T Rec. G.9904 [40]. With permission

of a MV/LV power transformation station. ITU-T Rec. G.9904 (PRIME) networks have a tree topology where the BN is the trunk. Every SN working has to get registered in the network by exchanging some information with the BN. To extend the range of ITU-T Rec. G.9904 (PRIME) networks, the BN can promote a SN from terminal node state to switch node state (proactive routing mechanism). A switch node is able

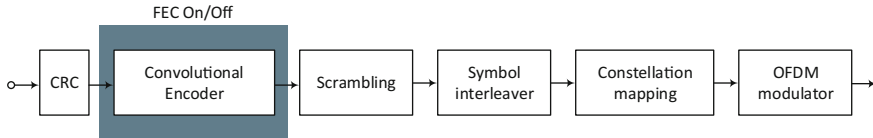


Fig. 4.15 Simplified structure of the ITU-T Rec. G.9904 (PRIME) transmitter. Adapted by the authors from ITU-T Rec. G.9904 [40]. With permission

to relay data to other nodes with no direct view of the BN. Every SN working as a switch represents a branch in the network topology.

The convergence layer (CL) allows to link different upper layer protocols to the MAC layer. In order to do it, the CL has been split into a Common Part Convergence Sublayer (CPCS) and Service-Specific Convergence Sublayer (SSCS). The CPCS provides segmentation and reassembly to all SSCS. ITU-T Rec. G.9904 (PRIME) specifies four SSCS: Internet Protocol version 4 (IPv4), Internet Protocol v6 (IPv6), IEC 61334-4-32, and NULL SSCS. A management plane, that allows local and remote management of nodes as well as a firmware upgrade mechanism, is also defined.

PHY layer

An OFDM-based PHY layer with 97 active carriers located in the CENELEC A band is defined. The sampling frequency is set to 250 kHz, and a 512-point discrete Fourier transform (DFT) is employed. No up-conversion is applied; hence, the baseband signal is directly injected into the power line. To this end, the DFT points have Hermitian symmetry. The cyclic prefix has 48 samples (192 μ s).

Figure 4.15 shows a simplified block diagram of the transmitter. As seen, it consists of a cyclic redundancy check (CRC) detecting code used to verify the integrity of the MAC service data unit (SDU). The forward error correction (FEC) consists of a convolutional code (CC) with rate $\frac{1}{2}$ and constraint length $K = 7$. The CC can be enabled or disabled on a per-frame basis. Then, an interleaver is applied to the bits transmitted in each symbol. Finally, the interleaved bits are mapped to one of the three differential phase shift keying (DPSK) modulations. These have the interesting particularity that the differential operation is applied in the frequency domain, instead of the conventional time domain one. This will be denoted as D_f PSK. Hence, the phase of the k th carrier depends on the phase of the $(k - 1)$ th carrier of the same symbol. Pilot carriers are introduced to provide a reference for the differential demodulation. Accomplishing the differential modulation in the frequency domain is intended to reduce the influence of the impulsive noise. However, it prevents from disabling carriers (or group of carriers) that experience bad channel conditions, which may significantly reduce the frame error rate (FER).

It is interesting to relate the system parameters with the channel characteristics described in Table 4.2. As shown there, 10% of the channels exhibit coherence bandwidths smaller than 2.28 kHz, which is 4.68 times larger than the carrier spacing $\Delta f = 488$ Hz. This condition is essential when a differential-in-frequency modulation

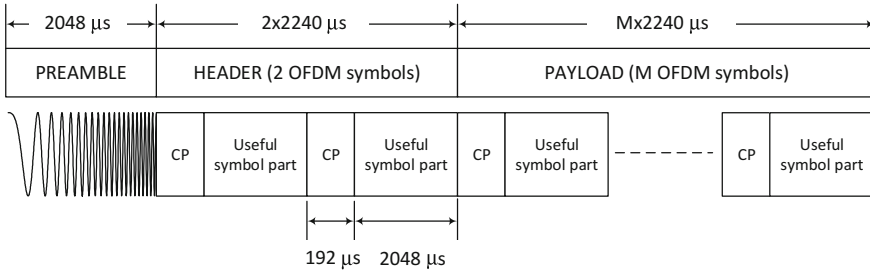


Fig. 4.16 Structure of the ITU-T Rec. G.9904 (PRIME) PHY layer frames. Adapted by the authors from ITU-T Rec. G.9904 [40]. With permission

is employed. Similarly, the cyclic prefix length is almost seven times larger than the delay spread of 90% of the channels. The significant length of the OFDM symbol (2240 μ s) is also much larger than most noise impulses, which reduces the influence of the latter in the performance. On the other side, the employed FEC seems to be excessively optimistic, since only a CC is employed.

Figure 4.16 depicts the structure of the PHY layer frames. As shown, they consist of a chirp signal, used as a preamble. It is mainly used for frame detection and automatic control gain adjustment. The preamble is followed by a 2-symbol header, which is always modulated using D_f BPSK and that conveys the payload length and the employed mode (modulation and FEC). It also contains the MAC header and the CRC. To provide increase robustness, 13 pilot carriers are employed in the header to supply the phase reference required for the differential demodulation. During the payload, a single carrier is used for this purpose. The maximum number of symbols of the payload is 63. It is interesting to relate the frame length with the mains period. Hence, the preamble and the header last for approximately 32.64% of a European mains cycle (20 ms), while the longest frame lasts for 7.38 mains periods.

Table 4.4 summarizes the main parameters of the PHY layer. The maximum bit rate of the PHY layer (assuming zero spacing between frames), denoted by R_b , can be computed as

$$R_b(\text{Mbit/s}) = \frac{96 \cdot M \cdot R \cdot 63}{2048 + (2048 + 192)(2 + 63)}, \quad (4.1)$$

where R is the code rate, which equals 1 if an uncoded transmission is employed, and $M = \{1, 2, 3\}$ is the number of bits/symbol of the employed modulation. The resulting values are shown in Table 4.5. These are slightly lower than other found in the literature, which do not take into account the preamble and the header length.

In order to assess the performance of a communication system, both the bit rate and the FER should be jointly compared. To this end, Fig. 4.17 shows the FER of the ITU-T Rec. G.9904 (PRIME) vs the SNR in an additive white Gaussian noise (AWGN) channel for both the coded and uncoded modulations. The SNR is measured at the DFT output. The aforementioned optimism of the FEC is reflected by the high

Table 4.4 Summary of the ITU-T Rec. G.9904 (PRIME) PHY layer parameters

Parameter	Value
Sampling frequency (kHz)	250
DFT size	512
Carrier spacing (Hz)	448
Used carriers	86–182 (97)
Used band (kHz)	41.99–88.87
Number of pilot carriers in the header/payload	13/1
Cyclic prefix length (samples/ μ s)	48/192
Modulations	D _f BPSK, D _f QPSK, D _f 8PSK
FEC	CC (K = 7, R = 1/2)
Interleaver	Per symbol
Preamble length (μ s)	2048
Header length (symbols/ μ s)	2/4480
Max payload length (symbols/ms)	63/141.12

Table 4.5 Maximum PHY layer bit rates of the ITU-T Rec. G.9904 (PRIME)

Modulation and FEC	PHY layer bit/rate (kbit/s)
D _f BPSK on/off	20.48/40.96
D _f QPSK on/off	40.96/81.92
D _f 8PSK _f on/off	61.44/122.88

SNR values required by the uncoded D_f8PSK (which is unlikely to be found in many actual channels) and also the relatively high SNR required by the most robust modulation,⁴ the coded D_fBPSK. It is worth to note that the uncoded D_fBPSK is needless because it achieves the same bit rate than the D_fQPSK but requires an SNR 4 dB higher.

MAC layer

This layer actually corresponds to the data link layer (DLL) of the open systems interconnection (OSI) model. As it has been said in the introduction, two kinds of devices are defined in the ITU-T Rec. G.9904 (PRIME) networks: the BN and the SNs. Every SN gets registered in the network by talking with the network BN. ITU-T Rec. G.9904 (PRIME) networks develop a tree topology, where the BN is the trunk. BN announces his presence by sending beacon messages (BPDU) at regular time intervals. When a SN boots up, it starts to listen for beacons; once it has been able to listen one or more beacons, a SN can send a request for registration in the network to the BN. In case no beacons are received during a certain amount of time, a SN can send a special MAC message called Promotion Needed (PNPDU). This PNPDU is

⁴Compared to the average SNR value of 7 dB derived in Sect. 4.2.2 and taking into account that all carriers use the same constellation and that the BER is dominated by the carrier with the lowest SNR.

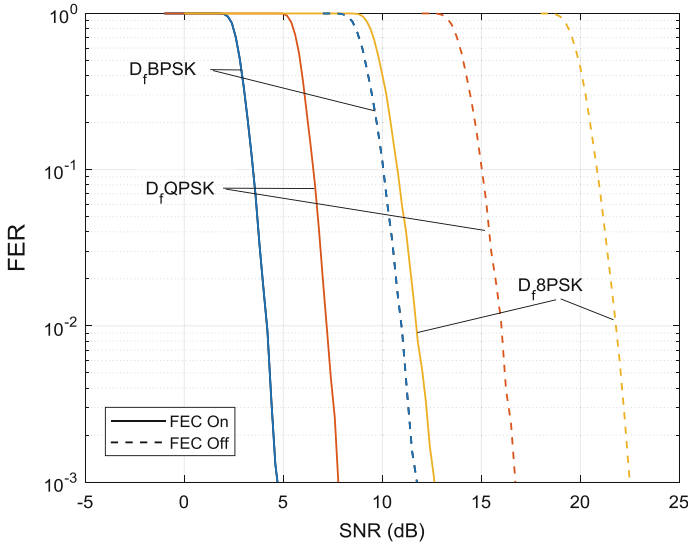


Fig. 4.17 FER of the ITU-T Rec. G.9904 (PRIME) PHY layer in an AWGN channel

received by all registered neighbor nodes and indicates that a SN is trying to connect to the network but has no direct view of the BN. The promotion to switch of one of the SN currently registered in the network is needed to bring connectivity to the connecting SN; this is the proactive routing mechanism chosen in the ITU-T Rec. G.9904 (PRIME).

The beacon presence in the medium establishes a time domain frame structure where Shared Contention Periods (SCP) and Contention-Free Periods (CFP) are defined. Each SN acting as a switch is able to extend this time frame structure sending beacons by itself in the network branches with no direct view to the BN. During the SCP, all nodes can access to the medium using a carrier sense multiple access with collision avoidance (CSMA/CA) algorithm to reduce collision probability. The BN may define a CFP, where medium access is arbitrated by it.

The ITU-T Rec. G.9904 (PRIME) specifies a mechanism to detect when a registered SN has left the network because of changes in the medium conditions or due to fatal errors it cannot recover from. As soon as a node registers in the network, it starts to exchange a kind of message with the BN called keep-alive messages (ALV). These messages are sent by each SN on a regular basis, and the absence of ALV messages from a SN helps the BN to be aware that the node is no longer present in the network.

The ITU-T Rec. G.9904 (PRIME) specification implements a connection-oriented communication mechanism. PRIME has defined several messages types at MAC level to open and close unicast, multicast, and broadcast connections. Unicast connections can be established between any pair of nodes, but generally in an AMI context most of the unicast connections will be established between the BN and

a SN. A unicast connection between two SNs is called “direct connection” and is defined separately in the standard. For multicast connections, a mechanism has been defined where the BN or any SN can join or leave a multicast group. Certain applications can require the BN to initialize a multicast group and then selectively invite some SNs to join the multicast group.

For unicast connections, an optional automatic repeat request (ARQ) mechanism has been defined. This optional ARQ works in an end-to-end basis. When a connection is established the negotiation of ARQ usage and the parameters associated to it is performed. A low-cost implementation of the ITU-T Rec. G.9904 (PRIME) can elide to implement the ARQ in order to save resources like memory or processing capabilities. ARQ windowing is supported with a maximum window size of 32.

CL layer

The CL is divided into two sublayers: the CPCS, that provides a set of generic services, and the SSCS, that provides specific services to each communication profile. There are several SSCSs, one per communication profile defined by the PRIME Alliance, but only one CPCS. The ITU-T Rec. G.9904 (PRIME) specifies SSCS for IEC 61334-4-32, IPv4, IPv6, and a NULL SSCS that provides a transparent path for MAC layer to upper layers. The most common SSCS used in AMI is the IEC 61334-4-32.

The main service provided by the CPCS is the segmentation and reassembly (SAR). Upper layers’ maximum transmission unit (MTU) may not be fitted into CL MTU and then need to be segmented⁵ by the CPCS.

Management Plane

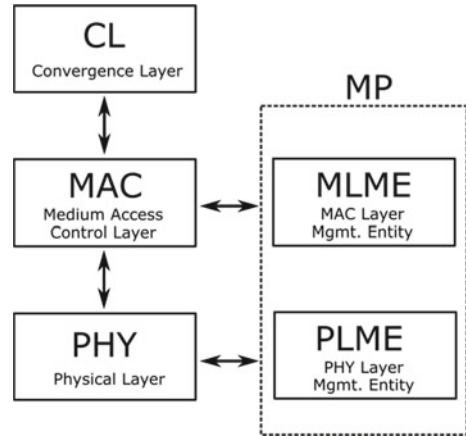
The management plane (MP) defined in the ITU-T Rec. G.9904 (PRIME) is an entity that provides management, configuration, and monitoring services to upper layers. Figure 4.18 shows the relationship of the MP to the remaining layers.

Main services provided by ML are node management (locally and remotely) and firmware upgrade. For node management, a set of attributes has been defined at the PHY and MAC layers. These attribute sets are called PLC information base (PIB) and are identified with a 16-bit value. This allows specifying up to 65535 PIB attributes. Identifiers (Ids) from 0 to 32767 are reserved for ITU-T Rec. G.9904 (PRIME) defined, PIBs but Ids from 32768 to 65535 are open for vendor specific usage. PIBs can be accessed and modified by upper layers through MP API, but the ITU-T Rec. G.9904 (PRIME) also defines mechanisms for remote PIB management from the BN; these mechanisms allow manipulating PIBs of any SN registered in a network from the BN of its network. In addition, a serial interface for PIB manipulation from an external device connected to the PRIME stack through a serial port is defined.

The ITU-T Rec. G.9904 (PRIME) has defined a protocol to enable the upgrading of the firmware related to the communication stack. It should be noted that an AMI meter could be simultaneously running different firmware; e.g., application and

⁵Segmentation means to break up a CPCS SDU into smaller pieces; each of these pieces or segments will be sent by MAC layer separately. At the end point of the communication (receiver node), all these segments are put back together to get a reassembled CPCS SDU.

Fig. 4.18 Management plane interaction with ITU-T Rec. G.9904 (PRIME) layers. Adapted by the authors from ITU-T Rec. G.9904 [40]. With permission



communications could be running in different processors. Due to this, a mandatory firmware upgrade process that must be able to upgrade the firmware for at least communication-related software is stated. This mechanism is compatible with an application-defined firmware upgrade process (i.e., DLMS/COSEM image transfer).

The firmware upgrade (FU) procedure specified in the ITU-T Rec. G.9904 (PRIME) allows launching a FU process from the BN and transferring a new firmware image to one or more SNs registered in the network. For that purpose, unicast and multicast modes have been specified, being the multicast mode optional. Firmware image integrity is checked by each SN involved in a FU process before applying it; in case of failure, a new image download can be requested. A mechanism for rejecting the new image after a “test” period is defined, allowing switching to the old version of the firmware if the new one does not work as expected.

4.2.3.2 PRIME v1.4

The industrial specification of PRIME v1.4 [56] was released in 2014 and has not been yet standardized by any standards developing organization (SDO). This section describes its enhancements with respect to the system defined in the ITU-T Rec. G.9904 (PRIME).

PHY layer enhancements

PRIME v1.4 includes two main PHY layer enhancements with respect to the ITU-T Rec. G.9904 (PRIME): bandwidth extension up to 500 kHz and two “robust modes”.⁶ Regarding the former, the frequency band 41.99–471.68 kHz is divided into eight channels separated by guard bands of 7.3 kHz, as shown in Fig. 4.19.

⁶The term “mode” refers to a particular combination of modulation and FEC and, in this case, also to a given frame structure.

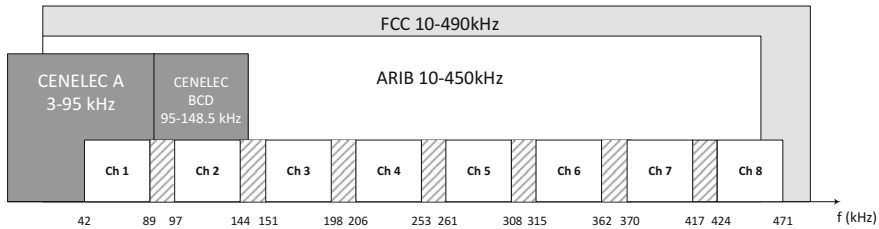


Fig. 4.19 Frequency bands and channel structure of PRIME v1.4. Adapted by the authors from PRIME Alliance TWG [55]

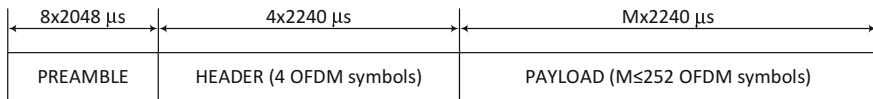


Fig. 4.20 Type B frame structure used in the robust modes. Reproduced from PRIME Alliance TWG [55]

Channels can be enabled or disabled on an individual basis. As seen, Channel 1 corresponds to the actual bandwidth used by ITU-T Rec. G.9904 (PRIME) transmissions. In fact, PRIME v1.4 includes a backward compatibility mechanism.

PRIME v1.4 defines two types of frames, named A and B. Type A frames have the same structure as the ITU-T Rec. G.9904 (PRIME) ones. Type B frames are employed in the so-called robust modes. As shown in Fig. 4.20, its preamble is four times longer than the one of the type A frames, and its header consists of four symbols, instead of two. Also, the payload may have up to 252 symbols. These symbols can be modulated using D_f BPSK or D_f QPSK, and the FEC consists of the CC employed in the normal modes plus a repetition code (RC) by 4. This stronger FEC is specific of the type B frames.

Since type B frames are not supported by ITU-T Rec. G.9904 (PRIME) devices, a backward compatibility mechanism is implemented in PRIME v1.4 to allow the coexistence of both devices in a mixed network. To this end, type B frames in the latter scenario are always prepended by the preamble and the header (with a predefined content) of a type A frame that will make ITU-T Rec. G.9904 (PRIME) devices to discard them.

Table 4.6 summarizes the PHY layer parameters. As seen, the carrier spacing and the cyclic prefix length are equal to the ones of the ITU-T Rec. G.9904 (PRIME), which have shown to be appropriate for the CENELEC A band. This is motivated by the need for ensuring backward compatibility with ITU-T Rec. G.9904 (PRIME). In the absence of this constraint, a shorter cyclic prefix might be more appropriate, because it would have improved the symbol rate while avoiding ISI and ICI, since channel response characteristics are better (lower delay spread and larger coherence bandwidth) in frequencies above 150 kHz.

Table 4.6 PHY layer parameters of PRIME v1.4

Parameter	Value
Sampling frequency (MHz)	1
DFT size	2048
Carrier spacing (Hz)	448
Number of pilot carriers per channel in the header/payload	13/1
Cyclic prefix length (samples/ μ s)	192/192
Modulations	D _f BPSK, D _f QPSK, D _f 8PSK
FEC	CC (K = 7, R = 1/2) in type A frames CC (K = 7, R = 1/2) + RC (4) in type B frames
Interleaver	Per symbol
Preamble length (μ s)	2048 (type A frames) 8 \times 2048 (type B frames)
Header length (symbols/ μ s)	2/4480 (type A frames) 4/8960 (type B frames)
Max payload length (symbols/ms)	63/141.12 (type A frames) 252/571.2 (type B frames)

Table 4.7 Maximum PHY layer bit rates of PRIME v1.4, where N_{ch} denotes the number of employed channels

Modulation and FEC	PHY layer bit/rate (kbit/s)
D _f BPSK robust	$5.22 \times N_{ch}$
D _f QPSK robust	$10.44 \times N_{ch}$
D _f BPSK on/off	$20.48 \times N_{ch}/40.96 \times N_{ch}$
D _f QPSK on/off	$40.96 \times N_{ch}/81.92 \times N_{ch}$
D _f 8PSK _f on/off	$61.44 \times N_{ch}/122.88 \times N_{ch}$

The values in Table 4.6 can be used to obtain approximate values of the maximum bit rate of the PHY layer (assuming zero spacing between frames). Results are given in Table 4.7, where N_{ch} denotes the number of employed channels.

Figure 4.21 depicts the FER of the PHY layer of PRIME v1.4 in an AWGN channel. Only coded modulations are shown. While the BER is independent of the number of channels, the FER is larger when using $N_{ch} = 8$ because the overall number of bits per frame increases. As seen, the robust mode using D_fBPSK reduces the SNR required to achieve a FER = 10^{-3} by about 5 dB with respect to the ITU-T Rec. G.9904 (PRIME).

MAC layer enhancements

A direct consequence of the PHY robust modes introduction is the frame enlargement and, consequently, the increase of the channel usage. Control messages sent in robust modes are up to four times longer. Hence, some improvements have been made at

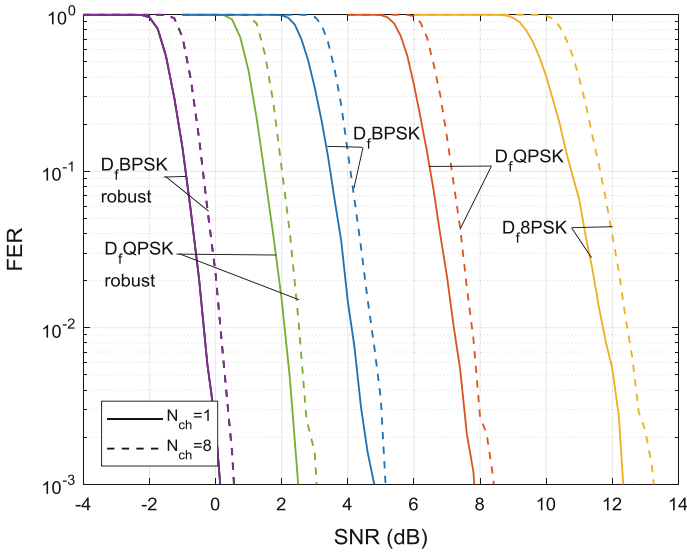


Fig. 4.21 FER of the PRIME v1.4 PHY layer in an AWGN channel

the MAC level in order to maintain the throughput, e.g., flexible MAC frame length and changes in the MAC frame structure to support different beacons lengths.

Some other changes introduced at the MAC level are an update of modulation selection algorithm in order to support robust modes, a simplification of multicast switching that avoids maintaining a multicast table to switch the appropriate multicast traffic in each node and a link level acknowledged keep alive mechanism.

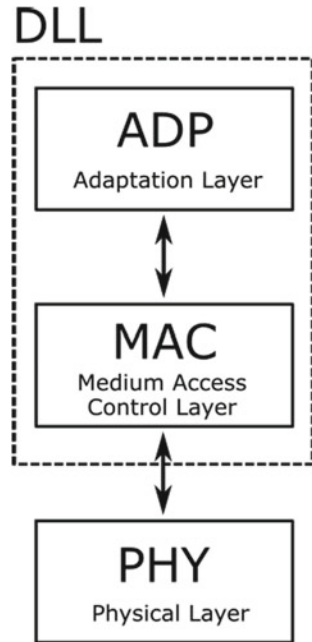
4.2.3.3 ITU-T Rec. G.9903 (G3-PLC)

G3-PLC was an open specification initially developed by Maxim Integrated Products for Electricité Réseau Distribuion France (ERDF), now Enedis. By 2011, the G3-PLC Alliance was founded to maintain and promote the specification. In 2012, it was standardized as ITU-T Rec. G.9903 [39], along with ITU-T Rec. G.9901 [37], which specifies the allowed PSD and the OFDM parameters to be used in each bandplan (used carriers, guard interval length, sampling frequency, etc.). The ITU-T Rec. G.9903 (G3-PLC) and its amendment were updated in 2014, 2015, and 2017, respectively.

The ITU-T Rec. G.9903 (G3-PLC) specifies the layers below IPv6 of an AMI system. Figure 4.22 shows its reference model.

An ITU-T Rec. G.9903 (G3-PLC) network is compounded of one or more domains named personal area network (PAN). A PAN is constituted by all nodes registered in that PAN, known as PAN devices. Each PAN device is uniquely identified by the

Fig. 4..22 ITU-T Rec. G.9903 (G3-PLC) reference model. Adapted by the authors from ITU-T Rec. G.9903 [39]. With permission



combination of the PAN identifier (PAN ID) and the address assigned to it known as short address (16-bit ID).

One of the nodes of the domain is assigned as PAN coordinator; the coordinator is responsible for admitting or denying access to the network and other management operations over the whole PAN, e.g., security keys management. A coordinator can also provide connectivity to other PANs or wide area networks (WANs).

An OFDM-based PHY layer with different bandplans, to allow operating in different regulated frequency bands, is employed. The MAC layer is based on the non-beacon-enabled mode of the IEEE 802.15.4 standard and is responsible for several tasks, such as medium access, message addressing, message integrity checking, message ciphering, data rate and tone-map negotiation, segmentation of large messages.

The adaptation sublayer (ADP) is the highest part of the DLL, and its role is to adapt the IPv6 layer frames to the IEEE 802.15.4 frame format [35]. The usage of IPv6 as Layer 3 protocol enables the use of the protocol ecosystem like transmission control protocol/user data protocol (TCP/UDP), simple network management protocol (SNMP), file transfer protocol (FTP) and the DLMS/COSEM transport layer over IP networks. This offers to the utilities a well-known set of standard protocols for the application layer.

PHY layer

The ITU-T Rec. G.9903 defines four bandplans named CENELEC A

(35.94–90.63 kHz), CENELEC B (98.44–121.86 kHz), FCC (154.69–487.5 kHz), and ARIB (154.60–403.125 kHz). The first two bandplans share most system parameters and so does the FCC and ARIB bandplans. In all cases, a pulse-shaped OFDM modulation is employed. Pulse shaping is intended to reduce the out-of-band emission. A 256-point DFT is used. Since no up-conversion is applied, the baseband signal is directly injected into the power line. To this end, the DFT points have Hermitian symmetry. OFDM symbols are prepended with a guard interval (GI) of 30 samples. Both symbol ends (eight samples at each side) are shaped with a raised cosine window and overlapped. Hence, the cyclic prefix reduces to 22 samples. The number of carriers used for conveying data depends on the bandplan. Their default values are given in Table 4.8. However, ITU-T Rec. G.9903 (G3-PLC) employs two useful features known as tone mask and tone map. The former refers to the set of tones that have no allocated power. It is a PAN-wide parameter that can be used to avoid interfering with other systems, such as the legacy NB-PLC ones defined in the ITU-T Rec. G.9901, or even to create cells using different sub-bands. Additionally, carriers used in the payload can be adaptively enabled/disabled on a group basis depending on their channel conditions. The tone map contains the set of carriers that convey no payload information.

Figure 4.23 shows the structure of the data frames. They consist of a preamble, a frame control header (FCH), and a payload. The preamble is formed by eight predefined OFDM symbols without GI, named SYNCP, plus $1 + 1/2$ symbols named SYNCM. The preamble is used for frame and symbol detection, automatic control gain adjustment, sampling frequency offset (SFO) estimation, and channel estimation (if the FCH or the payload are coherently modulated). The number of FCH symbols depends on the bandplan and on the number of masked carriers. The default values are given in Table 4.8. The FCH bits are always modulated using differential BPSK (DBPSK) in the CENELEC bandplans and BPSK (coherent) in the FCC and ARIB ones. Payload symbols can be differentially or coherently modulated, as indicated in Table 4.8. In the latter case, two additional symbols, named S1 and S2, are transmitted between the FCH and the payload. These are useful for SFO and channel estimation. For this purpose, a number of pilot carriers are transmitted using a comb-type arrangement in which the index of the pilot carriers varies from symbol to symbol.

Figure 4.24 depicts a simplified block diagram of the transmitter. As seen, a different FEC is applied to the FCH and to the payload. The FEC applied to the FCH consists of a CC with rate $1/2$ and constraint length $K = 7$ and a RC by 6. This is known as a super robust mode. The payload is encoded using a concatenated Reed-Solomon (RS) and a CC. A FEC scheme named robust mode additionally includes a RC by 4. In this case, the number of parity bits added by the RS is halved with respect to the normal mode. The robust mode is transmitted using DBPSK or BSPK. After the FEC, an interleaver is applied to the whole block of bits.

The output bits from the interleaver are mapped to any of the constellations indicated in Table 4.8. All payload carriers must employ the same constellation. As seen, both differential and coherent modulations are supported, although the latter

Table 4.8 PHY layer parameters of the ITU-T Rec.G.9903

Parameter	CENELEC A/B	FCC/ARIB
Sampling frequency (kHz)	400	1200
DFT size	256	256
Carrier spacing (Hz)	1562.5	4687.5
Used carriers	23–58 (36) 63–78 (16)	33–104 (72)/33–86 (54)
Used band (kHz)	35.94–90.63/98.44–121.88	154.69–487.50/154.69–403.13
Guard interval (samples/ μ s)	30/75	30/25
Cyclic prefix (samples/ μ s)	22/55	22/18.33
FCH modulation	DBPSK	BPSK
Payload modulations	DBPSK, DQPSK, D8PSK (optional BPSK, QPSK and 8PSK)	DBPSK, DQPSK, D8PSK ^a (optional BPSK, QPSK, 8PSK and 16QAM ^a)
Number of pilot carriers in the payload (when coherently modulated)	3/2 ^b	6/5 ^b
Number of carriers per tone-map sub-band	6	3
FEC FCH (data frames)	Super robust mode: CC (K = 7, R = 1/2) + RC(6)	
FEC payload	Normal mode: RS (255, 239 + CC (K = 7, R = 1/2) Robust mode: RS (255, 245) + CC (K = 7, R = 1/2) + RC(4)	
Interleaver	Per RS block	Per RS block
Preamble length (μ s)	6080	2026.67
FCH length (symbols) of the data frames	13/30	12/16
Max payload length (symbols)	252/252	511/511

^aNot supported in the ARIB bandplans

^bDefault tone mask assumed

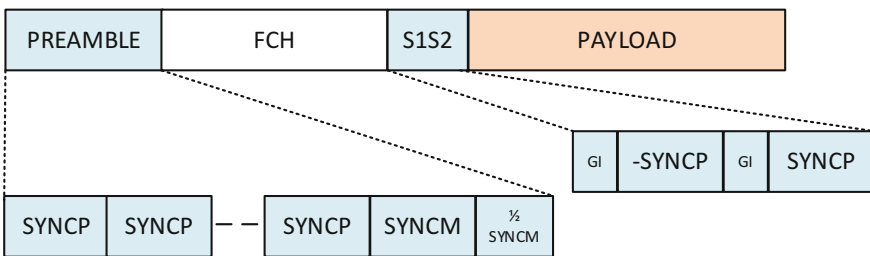


Fig. 4.23 Structure of the data frames of the ITU-T Rec. G.9903

are optional, except for the FCH of the FCC/ARIB bandplans, which are modulated using BSPK. Afterwards, a pre-emphasis function is applied. It allows shaping the PSD of the signal to compensate for the frequency selectivity of the channel. These,

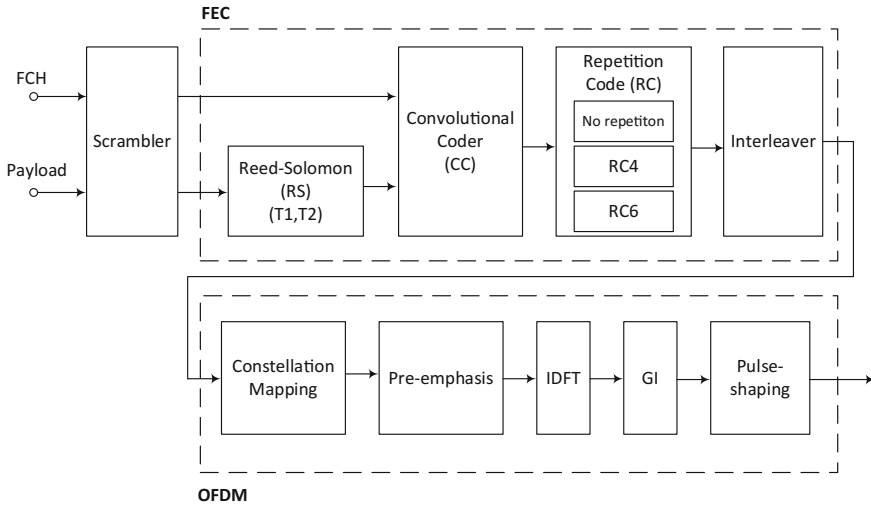


Fig. 4.24 Simplified structure of the ITU-T Rec. G.9903 (G3-PLC) transmitter. Adapted by the authors from ITU-T Rec. G.9903 [39]. With permission

along with the tone map, are very useful mechanisms to avoid the severe FER degradation that occurs in frequency-selective channels when all carriers are modulated using the same constellation. Then, symbols are applied to the IDFT, prepended with the GI and shaped with a raised cosine window.

Table 4.8 summarizes the PHY layer parameters of the ITU-T Rec. G.9903 (G3-PLC). It is interesting to relate these values with the channel characteristics described in Table 4.2. In 10% of the channels, both in the CENELEC A and the FCC bands, the carrier spacing is only 1.5 times lower than the coherence bandwidth. Similarly, the cyclic prefix length is only 1.97 times larger than the delay spread of 90% of the channels in the CENELEC A band and 1.7 times larger than the ones of the FCC band. Hence, ICI and ISI may be of importance in some channels. Interestingly, the employed FEC is much stronger than in the ITU-T Rec. G.9904 (PRIME), which reflects that a more pessimistic noise behavior is assumed.

In order to assess the performance of the ITU-T Rec. G.9903 (G3-PLC), both Table 4.9 and Fig. 4.25 are given. The former gives the maximum bit rates of the PHY layer (assuming no space between frames), and the latter depicts the FER in an AWGN channel for the CENELEC A and FCC bandplans. It shows two FER curves: ones in which only payload errors are taken into account (the FCH is assumed to be error-free) and others in which only FCH errors are considered. Interestingly, in the CENELEC A band, the FER of the payload when using robust BPSK is much better than the FER of the FCH. Hence, the latter will limit the performance. The main reason for this behavior is the bad performance of the DBPSK modulation employed in the FCH with respect to the BPSK used in the payload. In the FCC bandplan performance is also limited by the FCH FER but the difference with respect to the

Table 4.9 Maximum PHY layer bit rates of the ITU-T Rec. G.9903

Modulation and FEC	PHY layer bit/rate (kbit/s)	
	CENELEC A/B	FCC/ARIB
Robust mode differential	5.59/2.14	36.76/27.41
Robust mode coherent	5.05/1.81	33.51/24.71
DBPSK	19.97/9.46	106.15/85.31
BPSK	18.87/9.46	99.74/78.79
DQPSK	33.65/16.50	165.90/140.48
QPSK	32.08/14.73	159.49/131.53
D8PSK	44.55/21.71	207.64/176.55
8PSK	41.84/19.83	197.69/169.30

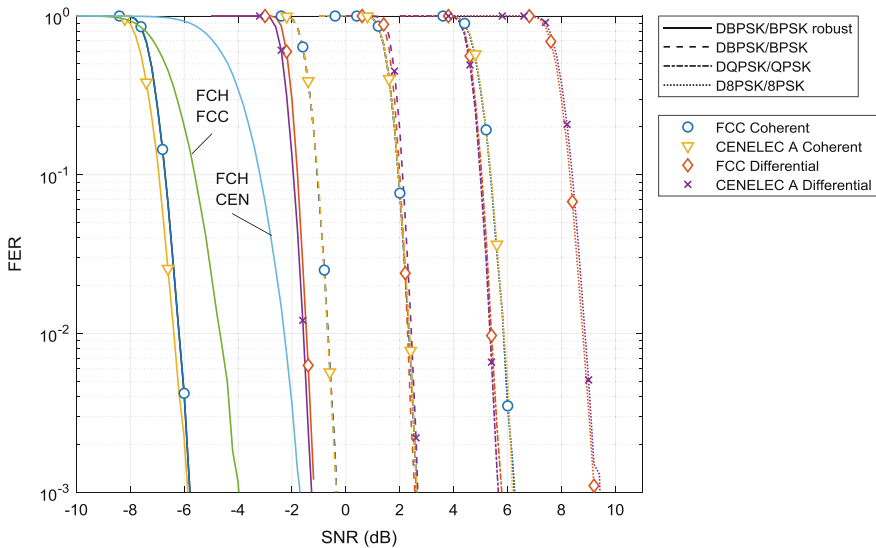


Fig. 4.25 FER of the ITU-T Rec. G.9903 PHY layer in an AWGN channel

robust BPSK is smaller than in the CENELEC A case. Since the same modulation is employed both in the FCH and the payload, the reason for this is the improved error correction capability of the RS. Finally, it can be seen that the coherent robust mode offers a 5 dB gain over the differential one. For the normal modes, the gain is about 3 dB.

Regarding the bit rates shown in Table 4.9, it must be highlighted that the values given by the differential modulations are slightly higher than the coherent. The reason for this is twofold. First, that the number of carriers used for conveying data is slightly lower when the payload is coherently modulated (because of the pilot carriers) and, second, because the additional S1 and S2 symbols introduced for SFO and channel estimation.

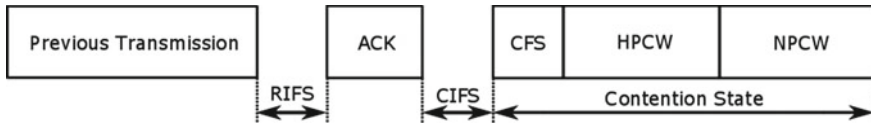


Fig. 4.26 Priority contention windows. Adapted by the authors from ITU-T Rec. G.9903 [39]. With permission

DLL

The ITU-T Rec. G.9903 (G3-PLC) splits the DLL into two sublayers:

- Medium access control sublayer (MAC) based on the IEEE 802.15.4 standard [35].
- IPv6 adaptation sublayer (ADP) based on IPv6 over Low-Power Wireless Personal Area Networks (6LoWPAN) [50] and its updates.

MAC Sublayer

As it has been said in the introduction, the MAC sublayer oversees several tasks that are going to be exposed in this section:

- Access to the medium,
- Message delivery assurance,
- Package ciphering,
- Data rate and tone-map negotiation, and
- Segmentation of large messages.

Regarding channel access, CSMA/CA with random back-off time is the selected algorithm. The random back-off time mechanism helps to reduce the probability of collision. Hence, when a node attempts to transmit a message, it has to wait for the beginning of next contention period (CP) taking into account the message priority; then, the node waits for the random back-off time, and if at the end of this back-off time the medium is found idle, the node will transmit the data. If the medium is found busy, the node has to wait for the next CP according to the message priority and the starts another random back-off period before trying to access the medium again. The random back-off time selection algorithm spreads the time over which a station attempts to transmit making use of an additive decrease multiplicative increase (ADMI) back-off mechanism.

Channel access prioritization is implemented by defining two levels of priority (high and normal) and two contention time windows during the contention state, as shown in Fig. 4.26. Three slots types are defined inside the CP; the first one is called contention-free slot (CFS) and is used to transmit subsequent segments of MAC packages without using the back-off mechanism to prevent possible interruption from other nodes, as it will be shown below. The second and third slots correspond to high priority contention window (HPCW) and normal priority contention window (NPCW). The MAC layer assigns messages to one of these contention windows (CWs) according to their priority.

Messages delivery and integrity is ensured by the use of mechanisms like MAC CRC and ARQ. When a node receives a MAC frame, it checks the MAC CRC of the message and acknowledges the frame in case of a correct reception. An acknowledge (ACK) frame is sent after the correct reception of a frame. The received frame correctness is determined by checking the MAC CRC. If a corruption is detected, the receiver can send a negative ACK (NACK), the originator will wait for a certain amount of time for the reception of the ACK, the absence of ACK, or the reception of an NACK causes a frame retransmission. The maximum number of retransmissions is determined by a MAC parameter (`macMaxFrameRetries`).

Frames segmentation is also a responsibility of the MAC sublayer. MAC MTU is 400 bytes but depending on the modulation these 400 bytes could not fit in a single PHY layer. When this occurs, segmentation is needed. If a MAC package must be segmented, the first segment is sent using the proper CW, but the subsequent segments are sent in the CFS, avoiding any other node to make use of the medium and simplifying the receptor resources needed for frame reassembly.

Another MAC sublayer key responsibility is to maintain an optimal link with neighbor nodes; this is accomplished by selecting the most suitable modulation and tone map for each neighbor node. Each MAC sublayer frame contains a flag called Tone-Map Request (TMR) that is set in the first frame a node sends to a new neighbor or when a timer expires (`TMRvalidtime`). When a node receives a MAC frame with TMS flag set, it must evaluate the quality of that link and select the modulation as well as the carriers to be used. Then, it must send to the originator a special MAC command called Tone-Map Response that contains all the parameters chosen by the receptor (modulation, tone map, etc.). On the reception of the tone-map response command, the originator updates the information about the link in his neighbor table, which is valid for a new `TMRvalidtime` period.

Security and data protection are based on the MAC security suite of IEEE 802.15.4 clause 7.6, which uses a cryptographic mechanism based on symmetric keys provided by higher layers. All nodes belonging a PAN share a group master key (GMK) that is used to cipher all MAC data messages if security is enabled. This GMK is distributed to the nodes in the bootstrap⁷ process and is responsibility of upper layer above G3-PLC to determinate how often and when it must be renewed.

Adaptation Sublayer

The ITU-T Rec. G.9903 (G3-PLC) uses IPv6 as network layer. The 6LoWPAN (IETF RFC 4944 and its updates) is employed as ADP to accommodate IPv6 frames to low-rate networks as the ones in IEEE 802.15.4. The main responsibilities of the ADP sublayer are IPv6 header compression (to save bandwidth), fragmentation and reassembly of large IPv6 frames, and discovery and registration of nodes in the network. Another important task is the implementation of an efficient routing protocol over 6LoWPAN that allows quick adaptation to link conditions and topology changes.

⁷Bootstrap process consists of the exchange of messages that allows a node to get registered in the network.

6LoWPAN is the result of a working group of the Internet Engineering Task Force (IETF). It defines encapsulation and header compression mechanisms to receive and transmit IPv6 packages over a IEEE 802.15.4 network. Reducing the amount of information transmitted to the minimum is vital for lossy networks like PLC ones. Hence, header compression is a powerful tool to optimize the physical medium. For example, a 48-byte IPv6 + UDP header can be compressed to only 2 bytes in certain conditions.

Another key responsibility of 6LoWPAN is to enable a mechanism for fragmentation and reassembly of IPv6 frames. This mechanism is needed to accommodate the MTU of IPv6 (1280 bytes) to the 400-byte MTU used in the ITU-T Rec. G. 9903 (G3-PLC). It is important to remark that the fragmentation procedure carried out by the ADP sublayer is independent of the segmentation process developed in the MAC layer. A large IPv6 package can be fragmented at ADP level, and each of these fragments could be segmented at MAC level depending on the link condition and the modulations selected on each hop of the network. While segmentation is a MAC process and each MAC package is segmented and reassembled hop by hop if needed, fragmentation is a process of the ADP sublayer and is performed end-to-end; hence, each fragment is treated as separated messages at MAC level and is only reassembled on the final destination of the message.

Efficient routing through the mesh network is another responsibility of the ADP sublayer. 6LoWPAN defines mechanisms for mesh routing management like the use of specific headers for package routing purposes (called mesh routing headers). Route discovery and maintenance are performed by means of the Lightweight On-demand Ad hoc Distance-vector Routing Protocol Next Generation (LOADng) [6].

LOADng is a reactive protocol that allows discovering and maintaining a set of routes to nodes in a 6LoWPAN network. The basic operation of LOADng consists in the generation of a route request (RREQ) message when a node needs to talk with another node and no route exists in the originator routing table. Every node receiving a RREQ forwards it until it reaches the final destination. The retransmission is performed in broadcast or unicast manner depending on the presence of the final destination in the routing table of the intermediate node. Once the final destination has received one or more RREQ through different paths, it evaluates the optimum route with the information accumulated in the propagation of RREQ messages and sends a route reply (RREP) in unicast through the optimal route.

Finally, the ADP sublayer is also responsible for discovering and authenticating nodes in the network. This task is accomplished by using the Extensible Authentication Protocol with Pre-Shared Key (EAP-PSK) [4]. Each node is able to execute a discovery process where it retrieves information about all the PANs to which it is able to communicate with. After that, the node can start a network join procedure with the PAN coordinator of the PAN it selects. During this process, the node and the coordinator authenticate each other and; if the authentication process succeeds, the PAN coordinator transfers the GMK to the node. All these procedures are based on the EAP-PSK protocol.

Table 4.10 Bandplans defined in the IEEE P1901.2

Bandplan	Frequency range (kHz)
CENELEC A	35.9375–90.625
ARIB 1	37.5–117.1875
FCC-Low	Same as ARIB 1
CENELEC B	98.4375–121.875
ARIB 2	154.6875–403.125
FCC-above-CENELEC	154.6875–487.5

Adapted by the author from [33]

4.2.3.4 IEEE P1901.2

Overview

The IEEE P1901.2 standard was approved by the IEEE Standards Association in 2013 [33]. Interestingly, one of its design aims was to be able to operate through MV/LV transformers. It defines the PHY and MAC layers of an HDR NB-PLC system operating in the frequency band up to 500 kHz. It is largely based on the ITU-T Rec. G.9903 (G3-PLC), to which the major difference is that the former does not define any routing algorithm. It includes some informative annexes. Of particular interest are Annex D, in which a channel model is proposed, and Annex E, in which an EMC measurement procedure and limits for the 150–500 kHz band, which is not specifically regulated in many countries (e.g., the EU), is given.

The reference model for the IEEE 1901.2 standard includes data and management planes. The data plane includes the DLL and the PHY. The defined DLL includes only the MAC sublayer. Examples for the ADP based on LOAD [6] or RPL (Winter et al. [67]) networks are included as annexes and are out of the scope of the standard. The management plane contains the MAC sublayer management entity (MLME) and the PHY layer management entity (PLME); both entities allow managing the MAC and PHY layers.

PHY layer

The PHY layer of the IEEE P1901.2 is almost equal to the ITU-T Rec. G.9903 (G3-PLC) one. Hence, this section does only describe their differences:

- Frequency bands. It defines the bandplans shown in Table 4.10.
- GI⁸: Two GI can be employed. The standard one, with 30 samples, as the one of the ITU-T Rec. G.9903 (G3-PLC), and an optional long GI with 52 samples supported in the FCC and ARIB bandplans.
- The FCH bits are coherently modulated (using BPSK) in all bandplans.
- The number of preamble symbols can be 9.5, as in the ITU-T Rec. G.9903 (G3-PLC), or 13.5.

⁸The IEEE P1901.2 refers to this field as cyclic prefix. However, since the symbol ends are windowed and overlapped, only part of the GI is actually a cyclic prefix.

- A super-ROBO mode is also defined for the payload. Its FEC consists of an RS code with 8 parity bytes, a CC, and RC by 6. The underlying modulation can be DBPSK or BPSK. The super-ROBO mode is optional in the CENELEC bandplans and mandatory in the remaining ones.
- An optional multi-tone mask mode is defined. In this mode, the employed frequency range is divided into sub-bands, each of them defined by a tone mask. A device can transmit on any of the sub-bands. This mode should be configured at deployment and is not interoperable with the default single-tone mask mode.

Although the IEEE P1901.2 and the ITU-T Rec. G.9903 (G3-PLC) PHY layers are not fully interoperable, e.g., in the latter the FCH is differentially modulated in the CENELEC bandplans, differences are so small that IEEE P1901.2 devices are expected to implement the interoperability profile with the ITU-T Rec. G.9903 (G3-PLC) defined in the specification.

MAC layer

The MAC layer of the IEEE 1902.1 is mainly based on the MAC layer of the ITU-T Rec. G.9903 (G3-PLC), which in turn is based on IEEE 802.15.4 specification. Both share the same definition for aspects like medium access, ARQ procedure, segmentation of frames and tone-map negotiation, and interframe spacing structure.

The only important difference between the ITU Rec. G.9903 (G3-PLC) and the IEEE 1901.2 is the definition of the optional multi-tone mask mode that can work in both the beacon-enabled and non-beacon-enabled modes.

4.2.3.5 ITU-T Rec. G.9902 (G.hnem)

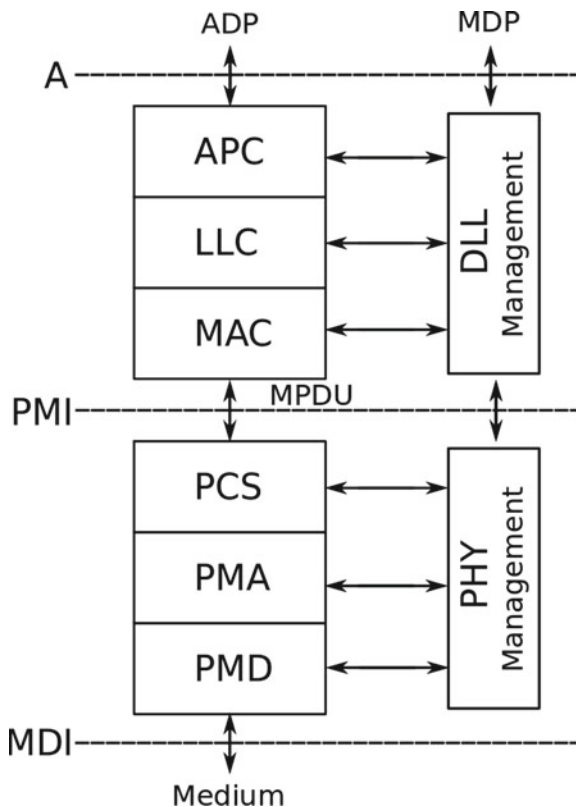
Overview

The ITU-T Rec. G.9902 (G.hnem) is aimed at supporting indoor and outdoor communications over LV and MV lines and through the MV/LV transformer [38]. It addresses a wide catalogue of smart grid applications like smart metering, communications between electric vehicles and charging stations, home automation.

The G.hnem reference model is shown in Fig. 4.27. It shows three reference points: application interface (A reference point), physical medium-independent interface (PMI) reference point, and medium-dependent interface (MDI reference point). Layers above the A reference point are beyond the scope of the G.hnem recommendation.

The A reference point represents the boundary between network layer (L3 in OSI model) and DLL layer. Its interface depends on the chosen network layer (IPv6, ethernet, etc.) . The sublayer in charge of providing an interface to the network layer is the application protocol convergence sublayer (APC). The logical link control sublayer (LLC) establishes, manages, resets, and terminates all connections with other nodes. It also ensures the quality of service (QoS) needed for each connection. Finally, the last sublayer of the DLL is the MAC; it coordinates the access to the medium by means of a CSMA/CA algorithm.

Fig. 4.27 ITU-T Rec. G.9902 (G.hnem) reference model. Adapted by the authors from ITU-T Rec. G.9902 [38]. With permission



The PMI reference point defines the boundary between the DLL and the PHY layers. The latter is divided into three sublayers: the physical coding sublayer (PCS), which provides bit rate adaptation between the MAC and the PHY layers as well as PHY-related control and management overhead. The physical medium attachment sublayer (PMA) provides forward error correction encoding and interleaving of the of the PHY frame content. Finally, the physical medium-dependent sublayer (PMD) modulates encoded PHY frames for transmission over the medium using OFDM symbols and demodulates the incoming PHY frames.

The ITU-T Rec. G.9902 (G.hnem) also defines a management interface used by upper layer to control the operation of the DLL and PHY layers.

An ITU-T Rec. G.9902 (G.hnem) network is composed of one or more logical domains. A domain is composed of all nodes registered in that domain. A node registered in a domain is identified by its domain ID and node ID. Each domain has a node that acts as a domain master (DM), which is in charge of performing admission, resignation, and other domain-wide operations. Different domains in the same network are connected by means of inter-domain bridges (IDB); this allows to nodes of different domains to communicate. It is also possible to connect to non-

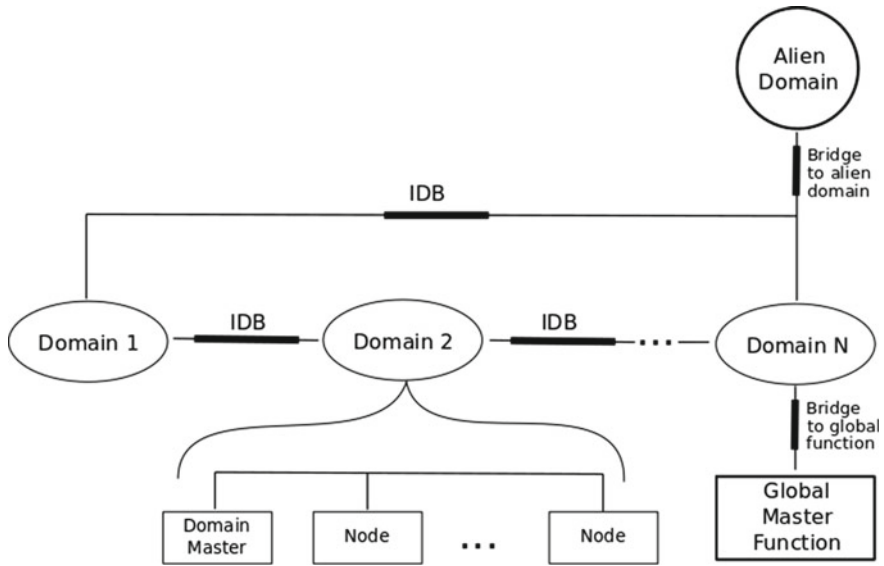


Fig. 4.28 Multiple domain ITU-T Rec. G.9902 (G.hnem) network example. Adapted by the authors from ITU-T Rec. G.9902 [38]. With permission

G.hnem “alien” domains. Figure 4.28 shows an example of a G.hnem network with different domains interconnected.

As mentioned, at the time of writing this chapter, there are no ITU-T Rec. G.9902 (G.hnem) compliant devices commercially available. A possible reason for this fact is that while the ITU-T Rec. G.9902 (G.hnem) defines a more powerful communication system than the remaining specifications, it is also the more complex one. Smart metering is the smart grid area that is currently focusing more deployment efforts, and the required reliability and data rates for this application can be provided by any of the aforementioned systems at a much-reduced price, which is a major concern for DSOs.

The unavailability of commercial devices makes it impossible to deploy an ITU-T Rec. G.9902 (G.hnem)-based network. Hence, the description of this standard will be much brief than the one of the ITU-T Rec. G.9903 (G3-PLC) and Rec. G.9904 (PRIME).

PHY layer

The ITU-T Rec. G.9902 (G.hnem) defines a pulse-shaped OFDM-based system which surprisingly (because of the low-working frequency range) uses up-conversion. It supports the bandplans given in Table 4.11, which also shows some system parameters associated with each of them. These values, along with the PSD limits, are defined in the ITU-T Rec. G.9901. Interestingly, the carrier spacing in the CENELEC band is equal to the one of the ITU-T Rec. 9903 (G3-PLC), while in the FCC bandplan it is 2/3 lower than its equivalent of the ITU-T Rec. 9903 (G3-PLC).

Table 4.11 Bandplans defined in the ITU-T Rec. G.9902 (G.hnem)

Bandplan	Frequency range (kHz)	IDFT size	Carrier spacing (Hz)	Guard interval (samples/ μ s)
CENELEC A	35.9375–90.625	128	1.5625	12/60 24/120 ^a
CENELEC B	98.4375–120.3125			
CENELEC CD	125–143.75			
FCC-1	34.375–137.5	256	3.125	24/20 48/40 ^a
FCC	34.375–478.125			
ARIB	34.375–418.85			
FCC-2	150–478.125			

^aUsed when the payload is modulated using 16-QAM

As seen, a larger GI is used when the payload is modulated using 16-quadrature amplitude modulation (QAM), which is the denser employed constellation. Doubling the GI is aimed at reducing the effect of the ISI and ICI.

PHY data frames have the following structure: a preamble, a common-part PHY frame header (PFH), two channel estimation symbols (CES), a variable-part PFH, and the payload. The preamble consists of N_1 OFDM symbols named S1 plus one—S1 symbol. Two values can be given to N_1 depending on the required robustness: 8 or $(8 + \text{ceil}[T_{\text{mains}}/(4T_{\text{OFDM}})])$, where $\text{ceil}[x]$ gives the nearest integer larger than x and T_{mains} and T_{OFDM} are the mains and the OFDM symbol period, respectively. The common-part PFH contains a set of fields that are common to all PHY frames, whereas the number of fields of the variable-part PFH depends on the type of frame. The number of OFDM symbols of both parts also depends on the bandplan. Remarkably, PFH symbols are transmitted without GI.

Regarding the employed modulations, there are two important differences with respect to the remaining HD NB-PLC systems described in this chapter. The first is that differential modulations are not employed: Only BPSK, 4-QAM, and 16-QAM are used. In order to improve the channel and SFO estimation obtained from the CES, pilot carriers are transmitted both in the PFH and the payload using a comb-type arrangement in which the index of the pilot carriers varies from symbol to symbol. The second is that carriers can be enabled/disabled on an individual basis, depending on the SNR. However, as in the remaining systems, the same modulation is employed in all carriers.

The employed FEC consists of a concatenated RS and CC. The former is equal to the used in the ITU-T Rec. G.9903 (G3-PLC), and two options exist for the latter: one with code rate 1/2 and another with rate 2/3. The RS is bypassed in short payloads and in the PFH to increase the efficiency. Encoded bits are passed to the interleaver, which splits them into fragments. These can be repeated a flexible number of times (2, 4, 6, or 12), depending on the required robustness. Then, one out of two available schemes are employed: interleave-over-fragment or interleave-over-AC-cycle. In the former,

the interleaver is applied to the aforesaid fragments. In the latter, each fragment is additionally repeated a number of times such that the resulting number of OFDM symbols spans over half mains cycle. This is specifically designed to combat periodic noise components which, as shown in subsection 4.2.2, have repetition patterns equal to half mains cycle. The aforementioned number of repetitions can be increased up to 32, 64, and 128 if the optional extremely robust mode is used.

The performance of ITU-T Rec. G.9902 (G.hnem) is almost unexplored. To the authors' knowledge, no publicly available results exist beyond the maximum data rates given in [23].

DLL

The DLL is in charge of MAC, retransmission and acknowledge, mesh networking, security and adaptation to upper layers.

Respecting to MAC, G.hnem employs a CSMA/CA algorithm with four priority levels. The highest priority level (level 3) is used for beacons and emergency data transfers, and the three lower priority levels (2, 1, and 0) are used for regular incoming application data. Management communications use the priority level 2 (highest level of application data priority).

A synchronized medium access has been defined as optional. If it is enabled, the DM periodically sends network beacons in a synchronous way. Each inter-beacon interval may include a number of contention-based and contention-free periods, similar to IEEE Std 802.15.4-2006 [35]. Participating nodes during a contention-based period use CSMA/CA for medium access.

The DLL is also in charge of upper layer frames segmentation. A “stop-wait-retransmit” mechanism has been chosen in order to reduce complexity in the nodes. A transmitter node is not allowed to transmit the next packet until all segments of the previous one are either positively acknowledged or timed out.

Mesh networking capability is a key functionality in most smart grid applications. G.hnem assumes that network layer (layer 3) routing will be used in the majority of IPv6 networks. Nevertheless in networks in which IPv6 routing is disabled, G.hnem specifies an optional DLL routing (layer 2 routing) that is switched off if layer 3 routing is enabled. The algorithm for L2 routing is still undefined.

Layer 2 security is provided by encryption and authentication of data and management frames exchanged between the nodes of the domain. The specified encryption method is based on the advanced encryption standard (AES) according to [48] and the counter mode with cipher block chaining message authentication code algorithm (CCM), according to [14]. The encrypted LLC frames are communicated using the CCM protocol (CCMP) that includes a CCMP header, the encrypted frame, and a message integrity code (MIC) for frame authentication. The CCMP header includes the necessary information for facilitating decryption.

G.hnem is designed to be able to manage different layer 3 protocols but IPv6 is the default one. Each layer 3 protocol has defined its own APC sublayer. The type of APC used by the transmitter is indicated in the packet header.

4.2.3.6 Performance Comparison

The performance of the HDR NB-PLC systems described in this chapter can be assessed at different layers. Three interesting ones are the PHY, MAC, and the application layers. Most of the results published in the literature are concerned with the ITU-T Rec. G.9904 (PRIME) and the ITU-T G.9903 (G3-PLC) standards. Since the IEEE P1901.2 is quite similar to the latter, some works do also include it, despite no commercially available devices exist. The number of studies that address the PRIME v1.4 specification is much more limited (due to its relative novelty), and to the authors' knowledge, no one includes the ITU-T G.9902 (G.hnem). The latter is somehow expected since not even a certification process has been already defined for this standard.

It is important to emphasize that significant performance differences may exist between different implementations (made by different manufacturers) of the same specification. Most of the PHY layer performance assessments are accomplished by means of simulations and implement an ideal PHY layer (e.g., no SFO and perfect channel estimation are usually assumed). However, the employed estimation algorithms and decoding strategy may significantly influence the performance. This also applies to the MAC layer, where manufacturers can implement techniques not defined in the standard, but compatible with it that may yield significant performance improvements [7].

The PHY layer performance of the ITU-T Rec. G.9904 (PRIME) and the ITU-T G.9903 (G3-PLC) in the CENELEC A band has been extensively studied by means of simulations using different channel models and experimentally in point-to-point configurations [26, 45, 47, 63, 68]. The IEEE P1901.2 is the most robust system, followed by the ITU-T Rec. G.9903 (G3-PLC) and, finally, the ITU-T G.9904 (PRIME). On the contrary, the latter attains higher data rates in benign channels [68]. Hence, it seems clear that the designers of these systems made different assumptions about the channel characteristics. While PRIME v1.4 is not included in the aforementioned comparisons, the FER curves given in this chapter suggest that its robustness is lower than the one of the ITU-T Rec. G.9903 (G3-PLC).

Results obtained in small field trials are also available [7, 53]. However, they are not useful for performance comparison because a single HDR NB-PLC system is involved. To this end, tests carried out in laboratory deployments by manufacturers of HDR NB-PLC devices are particularly interesting [7, 58]. Since the channel characteristics of these deployments are generally quite benign, they are particularly interesting for assessing the performance of the MAC layer and of the complete protocol stack. Interesting parameters for the high-level performance assessment of smart metering networks are the bootstrapping time (time for all the nodes to get registered), the average cycle time (time to read the energy consumption of all the nodes), the availability rate of each meter (the rate of successful meter reading attempts), and the maximum number of hops (number of times that a frame is relayed).

Results given in [7] assess the influence of the network topology on the application layer performance of two ITU-T G.9904 (PRIME) and PRIME v1.4-based smart metering networks deployed in a laboratory. Both networks consist of a BN and 112

Table 4.12 Performance values in the flat network when using ITU-T Rec. G.9904 (PRIME) devices

Base node vendor	Availability rate (%) [Number of meters with the given availability rate]	Average cycle time (min:s) [Standard deviation of the cycle time (s)]
Atmel	100 [112]	3:54 [9]
Other	100 [112]	7:25 [32]

Reproduced from Corchado et al. [7]

Table 4.13 Performance values in the multilevel network when using ITU-T Rec. G.9904 (PRIME) devices

Base node vendor	Availability rate (%) [Number of meters with the given availability rate]	Average cycle time (min:s) [Standard deviation of the cycle time (s)]
Atmel	100 [112]	13:07 [9]
Other	97.5 [1] 98.4 [4] 100 [107]	21:29 [46]

Reproduced from Corchado et al. [7]

smart meters. In one of them, referred to as flat network, all the meters have direct connection to the BN. In the other, named multilevel network, a set of attenuators are employed to create multiple levels of switching. Interestingly, the work also assesses the network performance when using two different BNs, one developed by Atmel (now Microchip Technology Inc.) and another manufactured by a different vendor.

Tables 4.12 and 4.13 summarize the results obtained when using ITU-T G.9904 (PRIME) devices in the flat and the multilevel networks, respectively. As seen, the average cycle time is strongly dependent on the network topology. The larger the number of hops, the larger the cycle time. It is also interesting to notice the significant influence of the employed BN on the performance. Hence, average cycle time differences of up to 47.4 and 38.9% exist in the flat and the multilevel networks, respectively. These important differences have a twofold cause. One is the MAC layer parameters selected by the vendors, which depend on the assumptions made about the network characteristics. The other is the use of some strategies that reduce the number of collisions. These are proprietary strategies compatible with the standard but not defined on it.

Table 4.14 Performance values in an ITU-T Rec. G.9903 (G3-PLC)-based smart metering network deployed in the laboratory using the CENELEC A band

Performance indicator	Value
Bootstrap time (min)	52
Average cycle time (min:s)	11:20

Reproduced from Sanz et al. [58]

The use of PRIME v1.4 (not shown in the tables) notably improves the performance. Hence, the average cycle time in the multilevel network falls from 13:07 to 9:27 (28% reduction), while the standard deviation remains almost equal (10 s).

Regarding the performance of ITU-T Rec.G.9903 (G3-PLC)-based smart metering networks, the study in [58] provides interesting results for the CENELEC A band. It assesses the bootstrap time and the average cycle time of a network deployed in a laboratory consisting of a coordinator and 100 nodes distributed in five levels, with a flat attenuation of 50 dB between each level. The tested network is quite similar (although not exactly equal) to the one in [7]. As shown in Table 4.14, the reported average cycle time is higher than the one reported in [7] for the PRIME v1.4-based network, but lower than the one of the ITU-T Rec. G.9904 (PRIME)-based network. Nevertheless, it should be taken into account that in both studies the channel is almost time-invariant. In these circumstances, routes from the BN/coordinator to each smart meter are quite stable. This somehow benefits the reactive routing algorithm used in the ITU-T Rec. G.9903 (G3-PLC) with respect to the proactive one used of the ITU-T Rec. G.9904 (PRIME). However, in an actual network, the rate of change of the noise characteristics might be in the order of the average cycle time. Hence, routes are expected to be much unstable.

Unfortunately, the performance in actual deployments is generally undisclosed by DSOs. Iberdrola, the Spanish DSO promoter of the PRIME Alliance, provides some of the few available results which, interestingly, also encompasses their BB-PLC-based MV backbone [3, 59, 62]. Reported values for the NB-PLC part are in agreement with the laboratory-measured ones described in this section.

4.3 Conclusion

Smart metering is the smart grid area that is currently focusing more deployment efforts. Power line communications (PLC) and radio frequency are the most widely used technologies for this purpose. The former is considered the most cost-efficient alternative, at least for scenarios where the number of customers connected to medium voltage to low voltage (MV/LV) transformers is large.

PLC systems can be classified according to the employed frequency band. Systems working in the range 3–500 kHz are referred to as narrowband (NB)-PLC, whereas the ones working in the range 1.6–250 MHz are referred to as broadband (BB) PLC.

The former is the most widespread PLC technology for connecting the smart meter to the MV/LV. While the latter can be also used for this purpose, in current smart metering deployments they are mainly used as a telecommunication backbone to connect the SS using the MV lines.

The EMC regulation that NB-PLC systems have to comply with depends on the region. Nowadays, the 3–95 kHz range, referred to as CENELEC A band, is used in the European Union (EU), while frequencies up to approximately 500 kHz are allowed in the USA and Japan. The utilized band determines the attainable bit rate and the capability of NB-PLC signals to cross MV/LV transformers, since the attenuation of the latter is lower in frequencies above 150 kHz.

NB-PLC technology has been used in smart metering applications for a long time. In the last decade, a set of systems, referred to as high data rate (HDR) NB-PLC, have been developed by different industrial alliances and standardization bodies. The most successful ones were initially specified by the PRIME and the G3-PLC alliances and lately standardized by the International Telecommunications Union (ITU) as ITU-T Rec. G.9904 and G.9903, respectively. The PRIME alliance has recently released an enhanced version named PRIME v1.4. These systems attain hundreds of kilobit/s in the frequency band up to 500 kHz and a few tens of kilobit/s in the band up to 95 kHz.

These HDR NB-PLC systems employ orthogonal frequency division multiplexing (OFDM) modulation in the physical layer and a Carrier Sense Multiple Access with Collision Avoidance (CSMA/CA) scheme at the medium access control (MAC) layer. Both implement a relay network controlled by a data concentrator that manages the network and that is located in the MV/LV transformer station. Smart meters can communicate with the data concentrator either directly or by means of other smart meters when the characteristics of the direct channel are too bad. Hence, the larger the number of smart meters connected to a data concentrator, the larger the availability rate.

The performance of HDR NB-PLC smart metering systems in actual deployments is generally undisclosed by DSOs. However, simulated and laboratory tests indicate that systems working in the CENELEC A band are able to retrieve the energy consumption of 100 smart meters in less than 15 min.

References

1. M. O. Ahmed, L. Lampe, Power line communications for low-voltage power grid tomography. *IEEE Trans. Commun.* **61**(12), 5163–5175 (2013)
2. I. Berganza et al., PLC for smart grid, in *Power Line Communications: Principles, Standards and Applications from Multimedia to Smart Grid*, ed. by L. Lampe, A.M. Tonello, T.G. Swart (Wiley, Chichester, 2016), pp. 509–561
3. I. Berganza et al., PRIME on-field deployment, in *Proceedings of the IEEE International Conference on Smart Grid Communications*, Udine, Italy, (2011)
4. F. Bersani, H. Tschofenig, in *RFC 4764: The EAP-PSK Protocol: A Pre-Shared Key Extensible Authentication Protocol (EAP) Method* (2007)

5. G. Chu, J. Li, W. Liu, Narrow band power line channel characteristics for low voltage access network in China, in *Proceedings of the International Symposium on Power Line Communications and its Applications (ISPLC)*, Austin, USA, (2013)
6. T. Clausen et al., in *IETF Internet-Draft: The Lightweight On-demand Ad hoc Distance-vector Routing Protocol—Next Generation (LOADng)* (2016)
7. J. A. Corchado et al., Application-layer performance analysis of PRIME in smart metering networks, in *proceedings of the IEEE International Conference on Smart Grid Communications (SmartGridComm)*, Sidney, Australia, (2016)
8. J. A. Cortés, L. Díez, F. J. Cañete, J. J. Sánchez-Martínez, Analysis of the indoor broadband power-line noise scenario. *IEEE Trans. Electromagn. Compat.* **52**(4), 849–858 (2010)
9. J. A. Cortés, A. Sanz, P. Estopiñán, J. I. García, Analysis of narrowband power line communication channels for advanced metering infrastructure. *EURASIP J. Adv. Signal Process.* **3**(4), 1–13 (2015)
10. J. A. Cortés, A. Sanz, P. Estopiñán, J. I. García, Performance Assessment of OFDM-based Narrowband PLC for Advanced Metering Infrastructure, in *Proceedings of the International Symposium on Power Line Communications and its Applications (ISPLC)*, Madrid, Spain (2016)
11. Directive 2004/108/EC, in *The European Parliament and of the Council of 15 December 2004 on the approximation of the laws of the Member States relating to electromagnetic compatibility and repealing Directive 89/336/EEC Text with EEA relevance* (2004)
12. Directive 2012/27/EU, in *The European Parliament and of the Council of 25 October on energy efficiency, amending Directives 2009/125/EC and 2010/30/EU and repealing Directives 2004/8/EC and 2006/32/EC, 2012/27/EU* (Brussels, Belgium, 2012)
13. DLMS User Association, <http://www.dlms.com/> (2017). Accessed 30 Dec 2017
14. M. J. Dworkin, *Recommendation for Block Cipher Modes of Operation: The CCM Mode for Authentication and Confidentiality* (NIST Special Publication 800–38C, USA, 2004)
15. Edison Electric Institute, *Smart Meters and Smart Meter Systems: A Metering Industry Perspective* (Edison Electric Institute, Washington, DC, 2011)
16. EN 500651:2011, in *Signalling on Low-Voltage Electrical Installations in the Frequency Range 3 kHz to 148.5 kHz Part 1: General Requirements, Frequency Bands And Electromagnetic Disturbances* (CENELEC, 2011)
17. EN 50561-1:2012, in *Power Line Communication Apparatus used in Low-Voltage Installations—Radio Disturbance Characteristics—Limits and Methods of Measurement—Part 1: Apparatus for in-Home Use* (CENELEC, 2012)
18. EN 50561-3:2016, in *Power Line Communication Apparatus Used in Low-Voltage Installations—Radio Disturbance Characteristics—Limits and Methods of Measurement—Part 3: Apparatus Operating Above 30 MHz* (s.1.:CENELEC, 2016)
19. EN 55022:2011, in *Information Technology Equipment—Radio Disturbance Characteristics—Limits and Methods Of Measurement* (CENELEC, 2011)
20. Engage Consulting Limited, in *High-level Smart Meter Data Traffic Analysis*, (2010)
21. FCC, in *Title 47 of the Code of Federal Regulations (CFR), Federal Communications Commission, Technical Report 47 CFR, 15, s.1.:s.n* (2008)
22. G3-PLC Alliance, in *Narrowband OFDM PLC specifications for G3-PLC Networks*, (2014)
23. S. Galli, J. Le Clare, Narrowband power line standards, in *MIMO Power Line Communications: Narrow and Broadband Standards, EMC, and Advanced Processing*, ed. by L.T. Berger, A. Schwager, P. Pagani, D. Schneider (CRC Press, Boca Raton, 2014), pp. 271–300
24. S. Galli, A. Scaglione, Z. Wang, For the grid and through the grid: the role of power line communications in the smart grid. *Proc. IEEE* **99**(6), 998–1027 (2011)
25. M. Giroto, A. M. Tonello, EMC regulations and spectral constraints for multicarrier modulation in PLC. *IEEE Access* **5**(3), 4954–4966 (2017)
26. M. Hoch, Comparison of PLC G3 and PRIME, in *Proceedings of the IEEE International Symposium on Power Line Communications and its Applications (ISPLC)*, Udine, Italy (2011), pp. 165–169
27. Homeplug, in *HomePlug AV White Paper*, (2005)

28. O. G. Hooijen, A channel model for the residential power circuit used as a digital communications medium. *IEEE Trans. Electromagn. Compat.* **40**(4), 331–336 (1998)
29. IEC 62056-5-3, in *DLMS/COSEM Application Layer*. (2017)
30. IEC 62056-6-1, in *Object Identification System (OBIS)*. (2017)
31. IEC 62056-6-2, in *COSEM Interface Classes*. (2017)
32. IEC, CISPR 16-1-1:2015, in *Specification for Radio Disturbance and Immunity Measuring Apparatus and Methods—Part 1-1: Radio Disturbance and Immunity Measuring Apparatus—Measuring Apparatus*. (2015)
33. IEEE P1901.2, in *IEEE Standard for Low-Frequency (less than 500 kHz) Narrowband Power Line Communications for Smart Grid Applications*. (2013)
34. IEEE P1901, in *IEEE Standard for Broadband Over Power Line Networks: Medium Access Control and Physical Layer Specifications*, (2010)
35. IEEE Std 802.15.4-2006, in *Wireless Medium Access Control (MAC) and Physical Layer (PHY) Specifications for Low-Rate Wireless Personal Area Networks (WPANs)*, (2006)
36. ITU-R SM.1879-2, in *The Impact of Power Line High Data Rate Telecommunication Systems on Radiocommunication Systems below 470 MHz*, (2013)
37. ITU-T Rec. G.9901, in *Narrowband Orthogonal Frequency Division Multiplexing Power Line Communication Transceivers—Power Spectral Density Specification*, (2014)
38. ITU-T Rec. G.9902, in *Narrowband Orthogonal Frequency Division Multiplexing Power Line Communication Transceivers for ITU-T G.hnem Networks*, (2012)
39. ITU-T Rec. G.9903, in *Narrowband Orthogonal Frequency Division Multiplexing Power Line Communication Transceivers for G3-PLC Networks*, (2017)
40. ITU-T Rec. G.9904, in *Narrowband Orthogonal Frequency Division Multiplexing Power Line Communication Transceivers for PRIME Networks*, (2012)
41. ITU-T Rec. G.9961, *Unified High-Speed Wireline-Based Home Networking Transceivers—Data Link Layer Specification*, (2015)
42. ITU-T Rec. G.9963, in *Unified High-Speed Wireline-Based Home Networking Transceivers—Multiple Input/Multiple Output Specification*, (2011)
43. ITU-T Rec. G.9960, *Unified High-Speed Wireline-Based Home Networking Transceivers—System Architecture and Physical Layer Specification*, (2015)
44. L. Jianming, Z. Bingzhen, G. Liang, Y. Zhou, Current situations and future developments of PLC Technology in China, in *Proceedings of the IEEE International Symposium on Power Line Communications and Its Applications*, pp. 60–65, Beijing, China, (2012)
45. M. Korki, C. Zhang, H. L. Vu, Performance evaluation of PRIME in smart grid, in *Proceedings IEEE International Conference on Smart Grid Communications*, Vancouver, Canada (2013)
46. L. Lampe, A.M. Tonello, T.G. Swart (eds.), *Power Line Communications: Principles, Standards and Applications from Multimedia to Smart Grid*, 2nd edn. (Wiley, Chichester, 2016)
47. J. Matanza, S. Alexandres, C. Rodríguez-Morcillo, Performance evaluation of two narrowband PLC systems: PRIME and G3. *Comput. Stand. Interfaces* **36**, 198–208 (2013)
48. F. P. Miller, A. F. Vandome, J. McBrewster, *Advanced Encryption Standard* (Alpha Press, Orlando, 2009)
49. R. R. Mohassel, A. Fung, F. Mohammadi, K. Raahemifar, A survey on advanced metering infrastructure. *Int. J. Electr. Power Energy Syst.* **63**, 473–484 (2014)
50. G. Montenegro, J. Hui, N. Kushalnagar, in *RFC 4944: Transmission of IPv6 Packets over IEEE 802.15.4 Networks*, (2007)
51. M. Nassar et al., Local Utility power line communications in the 3–500 kHz band: channel impairments, noise, and standards. *IEEE Signal Process. Mag.* **29**, 116–127 (2012)
52. OPERA Project, in *Deliverable 44: Report on Presenting the Architecture of PLC System, the Electricity Network Topologies, The Operating Modes and the Equipment over Which PLC Access System will be Installed*. s.l. The Open PLC European Research Alliance (OPERA) Consortium (2005)
53. V.N. Papilaya et al., Analysis of the Devolo's 500 kHz G3-PLC access technology based on smart grid field trials, in *Proceedings of the IEEE International Symposium on Power Line Communications and its Applications (ISPLC)*, Glasgow, UK, (2014)

54. PRIME Alliance TWG, in *Draft Specification for PowerLine Intelligent Metering Evolution R.1.3.6*. (2008)
55. PRIME Alliance TWG, in *PRIME v1.4 White Paper*. (2014)
56. PRIME Alliance TWG, in *Specification for PowerLine Intelligent Metering Evolution R.1.4.0*. (2014)
57. J. G. Proakis, *Digital Communications* (McGraw-Hill, Massachusetts, 1995)
58. A. Sanz, D. Sancho, C. Guemes, J. A. Cortés, A physical layer model for G3-PLC networks simulation, in *Proceedings of the IEEE International Symposium on Power Line Communications and Its Applications*, Madrid, Spain (2017)
59. A. Sendin et al., Performance results from 100,000+PRIME smart meters deployment in Spain, in *Proceedings of the IEEE International Conference on Smart Grid Communications (SmartGridComm)*, Beijing, China, (2012), pp. 145–150
60. A. Sendin, R. Guerrero, P. Angueira, Signal injection strategies for smart metering network deployment in multitransformer secondary substations. *IEEE Trans. Power Delivery* **26**(4), 2855–2861 (2011)
61. A. Sendin, I. Peña, P. Angueira, Strategies for power line communications smart metering network deployment. *Energies* **2014**(7), 2377–2420 (2014)
62. A. Sendin, J. Simon, I. Urrutia, I. Berganza, PLC deployment and architecture for smart grid applications in Iberdrola, in *Proceedings of the IEEE International Symposium on Power Line Communications and Its Applications*, Glasgow, UK (2014)
63. J. Slacik, P. Mlynek, R. Fujdiak, K. Dobesova, Experimental measurements of multi-carrier power line communication systems, in *Proceedings of the International Conference on Telecommunications and Signal Processing (TSP)*, Barcelona, Spain (2017)
64. STD-T84, *Association of Radio Industries and Businesses (ARIB), Power line communication equipment (10 kHz–450 kHz)*, (2002)
65. A. Sugiura, Y. Kami, Generation and propagation of common-mode currents in a balanced two-conductor line. *IEEE Trans. Electromagn. Compat.* **54**(2), 466–473 (2012)
66. N. Uribe-Pérez, L. Hernández, D. Vega, I. Angulo, State of the art and trends review of smart metering in electricity grids. *Appl. Sci.* **6**(3), 1–24 (2016)
67. T. Winter et al., in *RPL: IPv6 Routing Protocol for Low-Power and Lossy Networks*, (2012)
68. M. Wolkerstorfer et al., Measurement and simulation framework for throughput evaluation of narrowband power line communication links in low-voltage grids. *J. Netw. Comput. Appl.* **59**, 285–300 (2016)